Multi-parametric Analysis for Mixed Integer Linear Programming: An Application to Transmission Upgrade and Congestion Management

Jian Liu[1,2], Donald C. Wunsch II[2], Siyuan Wang[1,3], Rui Bo[1*]

[1]Department of Electrical and Computer Engineering, Missouri University of Science and Technology, Rolla, MO 65409, USA

[2]Kummer Institute Center for Artificial Intelligence and Autonomous Systems, Missouri University of Science and Technology, Rolla, MO 65409, USA

[3]Center for Energy, Environmental and Economic Systems Analysis (CEEESA), Argonne National Laboratory, Lemont, IL 60439

{[1,2]jliu@mst.edu, [2]dwunsch@mst.edu, [1,3]siyuan.wang@anl.gov, [1*]rbo@mst.edu}

Abstract: Upgrading the capacity of existing transmission lines is essential for meeting the growing energy demands, facilitating the integration of renewable energy, and ensuring the security of the transmission system. This study focuses on the selection of lines whose capacities and by how much should be expanded from the perspective of the Independent System Operators (ISOs) to minimize the total system cost. We employ advanced multi-parametric programming and an enhanced branch-and-bound algorithm to address complex mixed-integer linear programming (MILP) problems, considering multi-period time constraints and physical limitations of generators and transmission lines. To characterize the various decisions in transmission expansion, we model the increased capacity of existing lines as parameters within a specified range. This study first relaxes the binary variables to continuous variables and applies the Lagrange method and Karush-Kuhn-Tucker (KKT) conditions to obtain optimal solutions and identify critical regions associated with active and inactive constraints. Moreover, we extend the traditional branch-and-bound (B&B) method by determining the problem's upper bounds at each node of the B&B decision tree, helping to manage computational challenges in large-scale MILP problems. We compare the difference between the upper and lower bounds to obtain an approximate optimal solution within the decision-makers' tolerable error range. In addition, the first derivative of the objective function on the parameters of each line is used to inform the selection of lines for easing congestion and maximizing social welfare. Finally, the capacity upgrades are selected by weighing the reductions in system costs against the expense of upgrading line capacities. The findings are supported by numerical simulations and provide transmission-line planners with decision-making guidance.

Keywords: Transmission Planning; Parametric Analysis for MILP; Lagrangian Function; Branch and Bound; Unit Commitment and Economic Dispatch

	Sets	T_i^{off}	Minimum off (down) time for the *i-th* generator
N	Sets of buses, indexed by $i \in N$.	SD_i	Shutdown limit on Bus *i* (MW)
K	Sets of lines, indexed by $k \in K$.	DR_i	Ramp limit at Bus *i* (MW)
	Parameters		***Continuous variables***
C_{it}	Generation cost at Bus *i* in period *t* ($/MWh)	G_{it}	Generation dispatch of generator i in period t (MWh)
UC_{it}	Fixed cost to turn on generator *i* in period t ($/MWh)		***Binary variables***
SC_{it}	Start cost for generator *i* in period t ($/MWh)	U_{it}	1 if generator i is on in period *t*; else is 0
D_{it}	Demand at Bus i in period t (MWh)	V_{it}	1 if generator i starts up in period *t*, else is 0
GSF_{k-i}	Generation shift factor to branch k from Bus i		***Sensitivity parameters***
F_k^{max}	Transmission limit of branch k (MW)	θ_k	Transmission limit variety of branch *k* (MW)
G_{it}^{max}	Maximum power generation capacity at generator i in period t (MWh)		
SR_i	Startup ramp limit at Bus i (MW)		
UR_i	Ramp-up ramp limit at Bus *i* (MW)		
T_i^{on}	Minimum on (up) time for the *i-th* generator		

1. Introduction

The power industry is undergoing a significant transformation, driven by the pursuit of clean energy and zero carbon emissions. As a result, renewable energy now accounts for a substantial portion of the global electrical supply. By 2022, renewable sources like hydropower, wind, and solar energy accounted for 29.1% of the global electrical supply [1]. However, this rapid increase in renewable energy presents challenges such as volatility and supply-side uncertainty, exerting pressure on grid capacity and stability [2,3]. The inability of the grid to accommodate a power source with such characteristics can lead to many technical problems, such as line congestion, overvoltage, and stability issues [4]. Furthermore, with the increased demand for power, the capacities of the existing lines strain to keep up, resulting in line congestion. Uncertainties in renewable energy generation, consumer participation in load flexibility, and transmission capacity constraints can lead to sudden cost increases and jeopardize electricity procurement security.

To mitigate network congestion and ensure system security and stability, strategies such as demand response and transmission expansion planning (TEP) are implemented [5,6]. These strategies include upgrading the capacities of existing transmission lines and identifying new lines to be integrated into an existing electrical system [3,7,8]. Recent developments in this field have primarily focused on addressing uncertainties, such as those associated with wind turbine load and output power uncertainties. Notable research includes Ugranli and Karatepe's [9] TEP methodology that considers N-1 contingency conditions, Muñoz et al.'s [10] dynamic thermal level-based model to maximize line current capacity, and González et al.'s [11] analysis of how the community energy sector impacts power system expansion. Baldick and Neill [12] and Sebastian et al. [13] identified enhancing existing lines' capacity as a cost-effective alternative to building new ones, especially for renewable energy integration.

Given the changes in the power transmission system regarding planning and operation, Larruskain et al. [14] proposed achieving higher current densities in existing transmission lines to upgrade the transmission capacity. Increasing the power-carrying capability and reducing the conversion losses between AC (alternating current) distribution lines and DC (direct current) lines can significantly upgrade the transmission capacity [15,16,17,18]. Estimates suggest that by 2026, global investment in transmission and distribution infrastructure will reach $351 billion, with a portion allocated to eliminating line capacity restrictions [19]. Securing location approvals for new lines may extend project timelines; therefore, prioritizing the enhancement of existing lines' transmission capacity is crucial. Consequently, enhancing the transmission capacity of current lines is essential to meet the rising and unpredictable demands of renewable energy transmission cost-effectively, leveraging existing infrastructure to minimize new constructions costs. This research aims to develop a more suitable model for actual power grid operators or transmission planners to measure the effects of increased transmission capacity of existing lines.

This expansion, vital for congestion relief and both intra-regional and inter-regional power transmission, is often undervalued, particularly considering its resilience against the impacts of extreme weather on renewable energy generation [20]. According to research from the Lawrence Berkeley National Laboratory [21], existing transmission planning approaches run the risk of understating the economic value

of new transmission infrastructure. This is because extreme conditions and high-value hours, which account for only 5% of the time but contribute to approximately 50% of the transmission's value in alleviating congestion, are difficult to model and thus often overlooked in transmission planning.

There are various ways to alleviate line congestion, including line planning expansion and capacity enhancement [5,22,23]. However, practical methods to formulate the minimum cost function for increased transmission lines capacities during the entire grid are lacking. This study aims to create a practical model for power grid operators that quantifies the impact of increased line capacity. Using multi-parametric programming, the model provides precise solutions that analyze how enhanced transmission capacity reduce system costs and effectively alleviate line congestion.

Multi-parametric programming efficiently resolves the challenges presented, allowing adjustable parameter settings to enhance line transmission capacity. The parameter analysis produces an explicit affine formula for the investment of increasing the line capacity and decreasing system costs. Meanwhile, the changing range of line capacity on different lines is represented by different parameters, and this study discovers the cost-related parameter changes to select the most suitable line (s) for capacity adjustment by deriving the explicit system cost expressions obtained for each line with respect to parameter changes. In electricity markets, the independent system operator (ISO) aims to minimize system costs or maximize social welfare by efficiently managing energy clearance, reserves, and generator commitments [24,25]. In contrast to the previous power grid linear economic dispatch programming model [26,27,28,29], which focuses on demand uncertainty, this study includes a large number of binary variables in the security constrained unit commitment and economic dispatch (SCUCED) problem to better reflect the transmission capacity upgrade and ISO's goal of minimizing the system cost.

Contrasting with models that solve single-period problems [9,30,31,32], [33] explored constrained dynamic programming for multi-stage mixed-integer linear problems with linear objective functions. This study is characterized by a complex, multi-period, and multi-parametric mixed-integer linear programming (mp-MILP) model. Two methods for multi-parametric mixed-integer programming (mp-MIP) problems are iterating between two subproblems decomposed from the mp-MILP problem [34] and using the novel branch and bound algorithm [35]. However, the B&B method [36] may not effectively solve the problem when there are too many nodes/binary variables to explore because all possible nodes must be checked to determine the best solution, which increases the computational burdens of that task and makes this option impractical and unlikely.

To tackle the challenges associated with TEP, this study aims to answer two key questions: 1) How can an approximately affine solution be efficiently found for a multi-period and mp-MILP problem that considers transmission capacity uncertainty? 2) Given a cost budget, which transmission lines' capacity should be upgraded, and by how much, to increase societal welfare or reduce system costs? To address these questions, this study develops a right-hand side (RHS) parametric analysis MILP problem [37,38] by incorporating uncertainty parameters on the RHS of the capacity constraints of the transmission lines to capture their uncertain capacity. Our methodology involves solving the relaxed SCUCED problem to obtain

lower bounds, transforming continuous variables into binary ones to establish upper bounds, and comparing these bounds to find the best approximate solution within an acceptable error tolerance. This study is the first to use parametric analysis for mp-MILP to model TEP challenges, addressing the shortcomings of current transmission models that fail to handle uncertainty over multiple stages.

This study makes three significant contributions: First, by adding a time dimension to the left-side constraints matrix form used to represent the single-period programming problem, we first employ state-of-the-art modeling techniques and extend the single-period programming problem to the multi-period programming problem. To characterize the uncertainty in transmission expansion in this scenario, the domain of the parameter represents the existing line's increased capacity in each period. Then, we formulate the problem in matrix format and use the Lagrange function and the KKT condition to obtain the best solution at each node by relaxing the binary variables of unit commitment (UC) to continuous variables. This parametric analysis constructs a functional relationship between system costs and line capacity upgrades, advancing both theoretical methodologies and providing practical strategies for real-world energy systems management.

Second, multi-parameter programming problems with integer variables have exponential complexity, meaning that the computational burden and simulation time increase rapidly as the number of binary variables grows. Our proposed approach generates exact optimal analytical solution for small-scale mp-MILP parametric analysis problems and provides the best approximation analytical results for large-scale mp-MILP problems. We achieve this by calculating upper bounds (based on feasible integer solutions at each node) and lower bounds (achieved using the relaxed problem) at each node. Our dual-bound solution strategy significantly reduces the computational burden and accelerates the process. This method showcases substantial improvements over traditional techniques and underscores our commitment to enhancing both the efficiency and applicability of B&B algorithms in complex system environments.

Third, to adapt to changing operational conditions, such as increased demand and higher penetration of renewable energies, we advocate for strategic enhancements to transmission line capacity. This study investigates the functional relationship between reduced system costs and increased transmission capacity over multiple periods, using the RHS uncertainty of parametric analysis in ISO's SCUCED problem. By analyzing the first-order derivative of the objective function with respect to varying parameters, our method provides transmission line planners with a robust tool to optimize social welfare and minimize investment costs. This approach underscores the practical relevance of our theoretical innovations and makes a compelling case for their implementation in real-world energy system management scenarios.

The remainder of this paper is structured as follows: Section 2 reviews relevant studies. Section 3 establishes the model and formulates the transmission line capacity expansion problem from the perspective of the ISO, utilizing the SCUCED problem. Section 4 discusses RHS parametric analysis for large-scale MILP optimization. Section 5 illustrates the proposed approach by applying it to a single-period problem and multiple-period problems, including the IEEE-5 bus SCUCED and the IEEE-30 bus SCUCED. Finally, Section 6 summarizes the study and provides recommendations for further research. The supplementary

material of this paper contains several appendices. Detailed proofs, algorithmic procedures, and additional case studies are provided in the appendices.

2. Literature Review

This paper reviews the applications of multi-parametric programming models, approaches for solving mp-MIP problems, and the electricity market with uncertainty. Each of these topics is reviewed separately.

2.1 Multi-Parametric Programming Model

Dua et al. [34] introduced a model for engineering problems that treats control variables as optimization variables and state variables as parameters. This model addresses multi-parametric mixed-integer quadratic problems (mp-MIQPs) in mixed logical dynamical systems. In 2002, Dua et al. [39] applied the Lagrange method to solve multi-parametric quadratic problems (mp-QPs) and mp-MIQPs, characterized by convex and quadratic objective functions with linear constraints. They utilized an affine expression to systematically define parameter spaces, delineating optimality regions within model predictive and hybrid control contexts. In 2011, Gupta proposed a novel approach to multi-parametric programming that relies on enumerating active sets [40]. This method circumvents the combinatorial explosion typically associated with such enumerations and implicitly solves mp-QPs.

Habibi et al. [41] proposed a multi-parametric programming model to obtain explicit solutions to optimal control problems for certain classes of hybrid systems. They also developed an approximation algorithm for solving general types of mp-MILP problems. Avraamidou et al. [42] defined seasonal demand variability in supply chain planning problems as multi-parametric mixed-integer bi-level linear programming problems and proposed a novel algorithm that provided an exact, global, and parametric solution with or without demand uncertainty. Russo et al. [32] introduced a supervised learning framework to solve mp-MILP in Model Predictive Control. Fong et al. [30] presented a MILP approach for cost-effective and optimal deployment of base stations and repeaters.

Mate et al. [43] proposed an offline combinatorial approach to identify all active sets of constraints for the nonlinear model predictive control (MPC) problem by applying KKT conditions a priori. Mate [43] investigated KKT conditions to identify active constraints and presented piecewise affine control laws and the accompanying critical regions as part of the multi-parametric MPC technique for linear systems. Shokry et al. [44] analyzed multi-parametric programming to solve chemical process operation optimization problems with unavoidable Sensitivity parameters. Pappas et al. [45] examined an algorithm for the exact solution of explicit nonlinear MPC problems with convex quadratic constraints based on the second-order Taylor approximation of Fiacco's basic sensitivity theorem applied to an exact nonlinear MPC problem. Mahéo et al. [46] introduced a novel Benders decomposition framework for mixed-integer two-stage problems with uncertain recourse parameters.

Based on the above studies, multi-parametric programming models can address uncertainty problems in many fields. This study proposes an mp-MILP model in the multi-period electricity market to address

the challenges associated with the uncertainty of transmission line capacity in the SCUCED problem from the perspective of ISO, which contains binary variables reflecting the UC of generators; is mathematically characterized and yields an analytical solution.

2.2 MP-MIP Problems

Acevedo and Pistikopoulos [47] introduced a novel B&B algorithm that solves multi-parametric linear programs at each node of the search tree. This algorithm incorporates specialized bonding procedures to manage MILP problems with variable right-hand-side parameters. Dua and Pistikopoulos [48] decomposed the mp-MILP problem into two subproblems and then iterated between them. The first sub-problem was formulated as a multiple parametric linear programming (mp-LP) problem by fixing integer variables, and the second sub-problem was formulated as a MILP problem by relaxing the parameters as variables. Faísca et al. [49] developed a method for solving the mp-MILP problem by changing the parameters in the objective function and the RHS of the constraints, thus splitting the mp-MILP problem into two sub-problems: a master MINLP problem and a slave multi-parametric global optimization problem.

In the process of solving the mp-MILP, the mp-LP problem must be solved first. Gal and Nedoma [50] considered the computational aspects of the mp-LP problem and presented fundamental notations, theorems, and definitions; they demonstrated how to solve the mp-LP issue. Mitsos and Barton [51] introduced an enhancement of the well-known rational simplex approach for parametric LPs, which involved fewer successive operations on rational functions. Hladík [52] presented support set invariancy and optimal partition invariancy and compared them to the classical optimal basis approach for solving multi-parametric linear programming problems. Adelgren and Wiecek [53] suggested a new two-phase method to address the multi-parametric linear complementarity problem with sufficient matrices, where the mp-LCP solution was invariant over each region as a function of the parameters.

Crema [54,55] created a method for achieving a comprehensive multi-parametric analysis by solving a family of ILP problems and by selecting a suitable finite sequence of nonparametric MILP questions. Domínguez and Pistikopoulos [56] proposed two multi-parametric programming algorithms for handling pure-integer and mixed-integer bi-level programming problems, and the second algorithm targeted the mixed-integer case of the bi-level programming problem. Oberdieck et al. [35] proposed a new algorithm for solving mp-MILP problems that employ a B&B strategy and McCormick relaxation procedures to overcome the presence of bilinear terms in the model, thereby resulting in an envelope of parametric profiles containing the optimal solution to the mp-MILP problem.

This study specifies the combined constraints within matrix models, detailing both equality and inequality constraints comprehensively. Considering the uncertainty of transmission line capacity, this study proposes an effective approach for parametric analysis in multi-period MILP of ISO's SCUCED problem, which has not been addressed previously.

2.3 Uncertainty of Electricity Market

In the United States, both day-ahead and real-time electricity markets have a market-clearing process

modeled as a SCUCED problem [57,58]. Carrión and Arroyo [59] presented a new mixed-integer linear formulation that required fewer binary variables and constraints for the UC problem of thermal units. Lin et al. [60] described a transmission and distribution network coordinated dynamic economic dispatch (DED) model and proposed an efficient decentralized method to solve this problem using multi-parametric quadratic programming. Wang et al. [61] proposed a two-stage distributionally robust UC framework using both regular and flexible generation resources.

The resources for a wind-thermal DED problem fluctuate depending on the weather conditions [62]. Moarefdoost et al. [63] provided an alternative consideration for the uncertainty of renewable energy sources and the consequent ramping of conventional generation by a robust reformulation of the problem. Wind and solar availability are highly intermittent, resulting in uncertainty in demand fulfillment. The generation of these sources may differ according to the season and daily weather conditions. For example, temperature changes can lead to fluctuations in solar power output, and wind power generation can suddenly change with the wind speed variations [64]. Prajapati et al. [65] suggested the installation of an energy storage system to contend with the uncertainties caused by the unreliability of the power system owing to the high penetration of renewable energy sources.

From the perspective of the ISO, modeling and optimizing generators across multiple market-clearing processes with uncertainties and incomplete information, such as load demand, generate new challenges. Li [26] proposed an approach to eliminate the step change in the continuous locational marginal price curve regarding load fluctuation and smoothed the price curve step changes. Li and Bo [27] introduced a more efficient algorithm to identify new binding constraints and new marginal unit sets when the load increases. Vaskovskaya et al. [66] employed a nonlinear alternating current power system model to develop an analytical formula for expressing LMPs. Kara et al. [67] proposed a stochastic local flexibility market to solve grid issues, such as voltage deviations and grid congestion in distribution grids under demand uncertainty and random bidding processes.

TEP has been widely used to address network congestion in electricity markets and to ensure system security and stability. Building on the generation expansion planning framework by Lara et al. [68], Li et al. [69] proposed a MILP formulation for the Generation and Transmission Expansion Planning (GTEP) problem, which considers both generation and transmission upgrades. Georgiev et al. [70] proposed a risk-informed TEP method centered around an AC-based cascading failure model that simulates the power system responses after contingencies. The method aimed to provide an optimal expansion plan, striking a balance between the cost of expansion and the risk of systemic failures. Yin et al. [71] proposed a two-stage adaptive robust TEP model to address the limitations of existing models, which often overlook the temporal correlation among renewable energy outputs and fail to utilize extensive real-world data to reduce solution conservatism. This innovative model leverages a data-driven uncertainty set those accounts for spatio-temporal correlations. Meanwhile, Motta et al. [72] reviewed optimization approaches in the literature for integrating Demand Response into three critical areas of power systems planning: optimal power flow, UC, and generation and TEP. Furthermore, El-Meligy and Sharaf [73] designed a robust TEP model under long-term and short-term uncertainty to find the most cost-effective expansion plan while minimizing the highest

operation cost identified within a predetermined uncertainty framework.

Unlike previous research, this study first identifies congested lines by exploring the relationship between the optimal solution and uncertain line capacity parameters. Subsequently, we employ parametric analysis to assess the impact of transmission line capacity increases on optimization goals. Lines' capacity needing improvement is detected, and the suitable space for improvement is assessed, which boosts the social welfare of the system (i.e., maximizing social welfare through minimum investment).

3. Model Setup

To address the problem posed by the current transmission line upgrades, we develop a mp-MILP model aimed at minimizing ISO costs. Our model is based on assumptions drawn from previous work by Li [26], Li and Bo [27], and Vaskovskaya et al. [66]. See the following for the listed uses:

1) Each bus has one generator and one load for notational convenience.

2) The cost of electricity generation is assumed to be linear or piecewise linear, in accordance with electricity market rules.

With reference to previous studies, we construct the following mp-MILP model, which is a RHS mp-MILP model, detailed in Eq. (1):

$$\min \sum_{t=1}^{T}\sum_{i=1}^{N} C_{it}\times G_{it} + UC_{it}\times U_{it} + SC_{it}\times V_{it} \tag{1}$$

$$st.\begin{cases}
\sum_{i=1}^{N} G_{it} - \sum_{i=1}^{N} D_{it} = 0,\ t=1,2,\cdots,T;\ for\ i=1,2,\cdots,N & (1a)\\
\sum_{i=1}^{N} GSF_{k-i}\times\left(G_{it}-D_{it}\right) \le F_k^{\max}+\theta_k,\ \ t=1,2,\cdots,T;\ for\ k=1,2,\cdots K & (1b)\\
G_{it} - G_{i(t-1)} - (\mathrm{SR}_i - G_{it}^{\max})\cdot U_{it} - (UR_i - \mathrm{SR}_i)\cdot U_{i(t-1)} \le G_{it}^{\max},\ t=1,2,\cdots,T;\ for\ i=1,2,\cdots,N & (1c)\\
G_{it} - (G_{it}^{\max} - \mathrm{SD}_i)\cdot U_{i(t+1)} - \mathrm{SD}_i\cdot U_{it} \le 0,\ t=1,2,\cdots,T-1;\ for\ i=1,2,\cdots,N & (1d)\\
G_{i(t-1)} - G_{it} - (DR_i - SD_i)\cdot U_{it} - (SD_i - G_{it}^{\max})\cdot U_{i(t-1)} \le G_{it}^{\max},\ t=1,2,\cdots,T;\ for\ i=1,2,\cdots,N & (1e)\\
U_{it} - U_{i(t-1)} \le V_{it},\ t=2,3,\cdots,T & (1f)\\
\sum_{k=t-T_i^{on}+1}^{t} V_{ik} - U_{it} \le 0, t = T_i^{on}+1, T_i^{on}+2,\cdots,T & (1g)\\
\sum_{k=t-T_i^{off}+1}^{t} V_{ik} + U_{i(t-T_i^{off})} \le 1, t = T_i^{off}+1, T_i^{off}+2,\cdots,T & (1h)\\
G_{it}^{\min}\cdot U_{it} \le G_{it} \le G_{it}^{\max}\cdot U_{it},\ t=1,2,\cdots,T;\ for\ i=1,2,\cdots,N & (1i)\\
U_{it}\in\{0,1\}, the\ unit\ commitment\ for\ generator\ i\ in\ period\ t & (1j)\\
V_{it}\in\{0,1\}, the\ unit\ commitment\ for\ generator\ i\ at\ beginning\ of\ period\ t & (1k)
\end{cases}$$

where (1a) denotes the power balance constraint (i.e., energy supply matches the power demand). Eq. (1b) represents the transmission capacity limit on each line. Decision variables are constrained by startup ramp rates and ramp-up rates, as shown in Eq. (1c). Eqs. (1d) and (1e) impose constraints based on shutdown ramp rates and ramp-down rates on the current generation dispatch levels. The relationship between the

state of UC and the UC start state is shown in Eq. (1*f*). Eqs. (1*g*)–(1*h*) denote the minimum up and down time limits, T_i^{on} is the minimum on (up) time for the *i*-th generator, and T_i^{off} is the minimum off (down) time for the *i*-th generator. The constraint for the generation dispatch limit corresponding to UC for the *i*-th generator in the *t*-th period is denoted by Eq. (1*i*).

Unlike previous studies that applied multi-parametric linear programming to parametric analysis problems in various fields, our research specifically addresses uncertainties in transmission line capacities using an mp-MILP approach. Consequently, our proposed approach reveals an affine relationship between the objective function and changes in existing transmission line capacities with sensitivity parameters. In the scenario of adding new transmission lines to the existing system, the parameters domain represents the uncertain capacities of newly constructed lines.

4. Model Optimization and Analysis

To address the problem of RHS parametric analysis for mp-MILP, we employ a B&B method, considering previous studies [35,47]. The proposed algorithm and its related procedures are illustrated in Figure 1.

The algorithmic process for mp-MILPs is split into the following five steps. Section 4.1 describes step 0 for initialization. In Section 4.2, this study solves the fully relaxed problem, calculates the initial upper bound, and compares the optimal solution and the upper bound at the root node, representing step 1. Section 4.3 (step 2) describes selecting a branching variable and updating the set of nodes. Section 4.4 (step 3) determines whether the collection of nodes is empty. Section 4.5 (step 4) analyzes the process of solving and comparing the lower and upper bounds at every node. Section 4.6 (step 5) introduces the process to determine whether the Sensitivity parameter space is null. Finally, we summarize the application and insight for this proposed method in transmission network expansion and cost allocation in electricity markets.

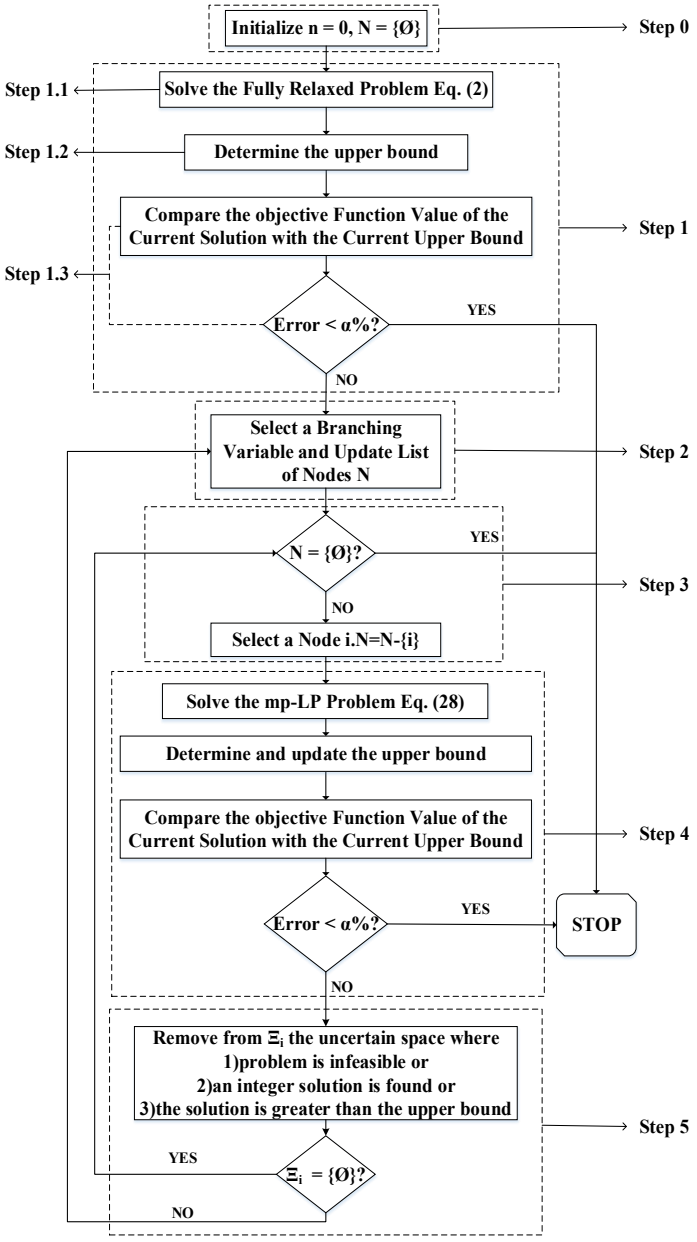

Fig.1: Algorithm for mp-MILPs

4.1 Initialization (Step 0)

First, initialize the collection of nodes that need to be solved, denoted as $N = \{\varnothing\}$, and record their counter $n = 0$.

4.2 Solve the fully relaxed problem and determine upper bound (Step 1)

4.2.1 Solve the fully relaxed problem (Step 1.1)

After initialization, we address the fully relaxed problem at the root node to discover the lower bound in the entire parameter space, as shown in Figure 1. In the fully relaxed problem, the binary variables are

relaxed to continuous variables with values ranging from 0 to 1. Consequently, the mp-MILP problem in Eq. (1) is transformed into an mp-LP problem (2).

$$\begin{aligned} &\min_{G,U,V} \sum_{t=1}^{T}\sum_{i=1}^{N} C_{it}\times G_{it} + UC_{it}\times U_{it} + SC_{it}\times V_{it} \\ &st.\begin{cases} Other\ constra\text{int}s\ are\ the\ same\ with\ (1a)\sim(1i)\ in\ (1) \\ 0\le U_{it}\le 1 \\ 0\le V_{it}\le 1 \end{cases} \end{aligned} \tag{2}$$

To simplify the problem in Eq. (2) and to facilitate the solution of subsequent problems, this study includes a matrix structure, as shown in Eq. (3)[1]:

$$\begin{aligned} &z = \min_{\omega} M^T\omega \\ &st.\begin{cases} A\omega \le b + \hat{F}^{\max} \\ H\omega = H\hat{D} \end{cases} \end{aligned} \tag{3}$$

Following the work of Oberdieck et al. [35], we combine the continuous variable representing power generation (economic dispatch) and the binary variable representing generator UC into a single matrix for the Lagrange Multiplier Method.

Several auxiliary submatrices are defined in Eq. (3), such as the matrix M, which is composed of three submatrices comprising all the coefficient information of the decision variables in the objective function.

$$\begin{aligned} M &= (C^T\ UC^T\ SC^T)^T_{1\times N(3T-1)} \\ &= \left(C_{11}\ C_{1T}\cdots C_{N1}\ C_{NT};UC_{11}\ UC_{1T}\cdots UC_{N1}\ UC_{NT};SC_{12}\ SC_{1T}\ SC_{N2}\ SC_{NT}\right)^T \end{aligned} \tag{3a}$$

In Eq. (3a), submatrix C^T, for example, has NT rows corresponding to the coefficient of the per-unit electricity generation cost for all generators in each period. Submatrix UC^T has NT rows corresponding to the fixed cost coefficients of UC. Submatrix SC^T has N(T-1) rows corresponding to the coefficient of the startup cost in the objective function.

We define three vectors: D, G, and U, each with NT rows and 1 column. Here, D represents the demand for each bus in each period (e.g., D_{11} indicates the demand for bus 1 at period 1), G represents the generation dispatch decision variables, and U represents the UC decision variables. The startup or shutdown status of each generator is represented by V, which is an N(T-1) row and 1 column vector.

$$\begin{cases} D = \left(D_{11}\cdots D_{1T}\cdots D_{N1}\cdots D_{NT}\right)^T_{1\times NT} \\ G = \left(G_{11}\cdots G_{1T}\cdots G_{N1}\cdots G_{NT}\right)^T_{1\times NT} \\ U = \left(U_{11}\cdots U_{1T}\cdots U_{N1}\cdots U_{NT}\right)^T_{1\times NT} \\ V = \left(V_{12}\cdots V_{1T}\cdots V_{N2}\cdots V_{NT}\right)^T_{1\times N(T-1)} \end{cases} \tag{3b}$$

Utilizing the aforementioned vectors, this study defines a new vector ω, detailed in Eq. (3c), consisting of three sub-vectors: G, U, and V.

[1] In this study, if T is the right superscript of a matrix or vector, it means transpose; otherwise, it means the end of the optimization period.

$$\omega = (G\ U\ V)^{T}_{1\times N(3T-1)} \tag{3c}$$

Note that A is the left-side coefficient matrix for all the inequality constants in Eq. (2), which includes $KT+12NT-4N-\sum_{i=1}^{N}(T_i^{on}+T_i^{off})$ rows and $N(3T-1)$ columns. The zero elements in the first row indicate that zero matrices are required to keep A intact. The diagonal submatrices are minus one element and one element, respectively. For simplicity, we use (Num) in the subscript to represent $KT+12NT-4N-\sum_{i=1}^{N}(T_i^{on}+T_i^{off})$ (Appendix A provides a detailed summary of matrix A).

$$A=\begin{pmatrix} GSF & 0 & 0 \\ ramp\ up & & \\ shut\ down & & \\ ramp\ down & & \\ state\ transition & & \\ \min on & & \\ \min off & & \\ -1 & \hat{G}^{\min} & 0 \\ 1 & -\hat{G}^{\max} & 0 \\ 0 & -1 & 0 \\ 0 & 1 & 0 \\ 0 & 0 & -1 \\ 0 & 0 & 1 \end{pmatrix}_{Num\times N(3T-1)} \tag{3d}$$

In Eq. (3e), b and $\hat{F}^{\max}$ are vectors with Num rows and 1 column, consisting of elements that are either ones or zeros, representing specific coefficients in the constraints.

$$\begin{cases} b=\left(GSF\cdot D\ \ G_i^{\max}\ \ 0\ \ G_i^{\max}\ \ 0\ 0\ 1\ 0\ 0\ 0\ 1\ 0\ 1\right)^{T}_{1\times Num} \\ \hat{F}^{\max}=\left(F^{\max}+\theta\ \ 0\ 0\ 0\ 0\ 0\ 0\ 0\ 0\ 0\ 0\ 0\ 0\right)^{T}_{1\times Num} \end{cases} \tag{3e}$$

In Eq. (3f), θ and $F^{\max}$ are row vectors with KT rows and 1 column. The element in θ denotes the uncertainty parameter for each line, which also indicates the possible enhanced capacity. The current maximum capacity of the lines is denoted by $F^{\max}$.

$$\begin{cases} F^{\max}=\left(F_1^{\max}\ \cdots F_1^{\max}\ \ F_2^{\max}\ \cdots F_2^{\max}\ \cdots F_K^{\max}\ \cdots F_K^{\max}\right)^{T}_{1\times KT} \\ \theta=\left(\theta_1\ \cdots \theta_1\ \ \theta_2\ \cdots \theta_2\ \cdots \theta_K\ \cdots \theta_K\right)^{T}_{1\times KT} \end{cases} \tag{3f}$$

Using Eq. (3), we derive the matrix structure requirements for the equality constraints from matrix H, which consists of T rows and N(3T-1) columns. Eq. (4a) is used to present $H\omega$, and Eq.(4b) denotes $H\hat{D}$:

$$H\omega=\begin{pmatrix} \underbrace{1\cdots0}_{|N|} & \underbrace{1\cdots0}_{|N|} & \cdots\cdots\cdots & \underbrace{1\cdots0}_{|N|} & \underbrace{0\ \cdots\cdots\cdots\ 0}_{} \\ \underbrace{0\ 1\cdots0}_{|N|} & \underbrace{0\ 1\cdots0}_{|N|}\cdots & \underbrace{0\ 1\cdots0}_{|N|} & 0\ \cdots\cdots\cdots & 0 \\ \vdots & \vdots & & & \vdots \\ \underbrace{0\cdots1}_{|N|} & \underbrace{0\cdots1}_{|N|} & \cdots\cdots\cdots & \underbrace{0\cdots1}_{|N|} & \underbrace{0\ \cdots\cdots\cdots\ 0}_{N(2T-1)} \end{pmatrix}_{T\times N(3T-1)} \begin{pmatrix} G \\ \bar{U} \\ V \end{pmatrix}_{N(3T-1)\times 1} =\left(\sum_{i=1}^{N} G_{it}\right) \tag{4a}$$

$$H\hat{D}=\begin{pmatrix} \underbrace{1\cdots0}_{|N|} & \underbrace{1\cdots0}_{|N|} & \cdots\cdots\cdots & \underbrace{1\cdots0}_{|N|} & \underbrace{0\ \cdots\cdots\cdots\ 0}_{} \\ \underbrace{0\ 1\cdots0}_{|N|} & \underbrace{0\ 1\cdots0}_{|N|}\cdots & \underbrace{0\ 1\cdots0}_{|N|} & 0\ \cdots\cdots\cdots & 0 \\ \vdots & \vdots & & & \vdots \\ \underbrace{0\cdots1}_{|N|} & \underbrace{0\cdots1}_{|N|} & \cdots\cdots\cdots & \underbrace{0\cdots1}_{|N|} & \underbrace{0\ \cdots\cdots\cdots\ 0}_{N(2T-1)} \end{pmatrix}_{T\times N(3T-1)} \begin{pmatrix} D \\ 0 \end{pmatrix}_{N(3T-1)\times 1} =\left(\sum_{i=1}^{N} D_{it}\right) \tag{4b}$$

In this model, the original problem in Eq. (3) can be rewritten as follows:

$$\min_{\omega} M^T\omega \quad st.\ \begin{cases} A\omega-b-\hat{F}_{\max}\le 0 \\ H\omega-H\hat{D}=0 \end{cases} \tag{5}$$

Based on Eq. (5), the constraints are drawn as follows, assuming $g_i(\omega)$ denotes an inequality constraint and $h_j(\omega)$ stands for an equality constraint.

$$\begin{cases} g_i(\omega)=A_i\omega-b_i-\hat{F}_i^{\max} \\ h_j(\omega)=H_j\omega-H_j\hat{D} \end{cases} \tag{6}$$

Here, the subscripts i and j denote the *i*-th and *j*-th rows of the corresponding matrices, respectively. The formulas in Eq. (5) in the following form in accordance with the Lagrange method are used:

$$\begin{cases} L=f(\omega)+\sum_{i=1}^{Num}\mu_i\cdot g_i(\omega)+\sum_{j=1}^{T}\lambda_j h_j(\omega) & (7) \\ f(\omega)=M^T\omega & (7a) \\ g(\omega)=A\omega-b-\hat{F}^{\max}\le 0 & (7b) \\ h(\omega)=H\omega-H\hat{D}=0 & (7c) \end{cases}$$

Considering that ω^* is the optimal solution to the problem, the best response function (i.e., the first-order derivative function) of Eq. (7) is shown as follows:

$$\frac{\partial L}{\partial \omega}=\frac{\partial f(\omega^*)}{\partial \omega}+\sum_{i=1}^{Num}\mu_i\cdot\frac{\partial g_i(\omega^*)}{\partial \omega}+\sum_{j=1}^{T}\lambda_j\cdot\frac{\partial h_j(\omega^*)}{\partial \omega}=M+A^T\mu+H^T\lambda=0$$

$$where,\ \begin{cases} f(\omega^*)=M^T\omega^*, \nabla f(\omega^*)=M \\ g_i(\omega^*)=A_i\omega^*-b_i-\hat{F}_i^{\max}, \nabla g(\omega^*)=A^T \\ h_j(\omega^*)=H_j\omega^*-H_j\hat{D}, \nabla h(\omega^*)=H^T \end{cases} \tag{8}$$

Based on the KKT conditions, the following findings are produced:

$$\begin{cases} \nabla_x L=\partial L/\partial\omega=0\Rightarrow M+A^T\mu+H^T\lambda=0 \\ \nabla_{\lambda_j} L=\partial L/\partial\lambda_j=0\Rightarrow H\omega-H\hat{D}=0, j=1,2,\ldots,T \\ g_i(\omega)=A_i\omega^*-b_i-\hat{F}_i^{\max}\le 0, i=1,...,Num \\ \mu_i\ge 0,\ i=1,2,\ ...,Num \\ \mu_i g_i(\omega)=\mu^T(A\omega-b-\hat{F}^{\max})=0, i=1,...,Num \end{cases} \tag{9}$$

Using the second and fifth lines of Eq. (9) yield:

$$\begin{cases} \mu^T(A\omega-b-\hat{F}^{\max})=0 \\ \lambda^T(H\omega-H\hat{D})=0 \end{cases} \tag{10}$$

Let $Y=\begin{pmatrix}A\\H\end{pmatrix}$, $N=\begin{pmatrix}b+\hat{F}^{\max}\\H\hat{D}\end{pmatrix}$, $Lm=\begin{pmatrix}\mu\\\lambda\end{pmatrix}$, and Eq. (10) be combined as

$$\boldsymbol{Lm^T(Y\omega-N)=0} \tag{11}$$

The best solutions of the convex LP problem are always located at the vertices of its feasible region; hence, matrix Y is split into two submatrices, Y_p and Y_s, where Y_p is the matrix containing all active constraints and Y_s is the matrix containing all inactive constraints. N_p and N_s are RHS terms of the corresponding constraints of Y_p and Y_s, respectively. Eq. (11) can be expressed as follows:

$$Lm_p^T\left(Y_p\omega-N_p\right)=0 \tag{12a}$$

$$\boldsymbol{Lm_s^T\left(Y_s\omega-N_s\right)=0} \tag{12b}$$

For the active constraints in Eq. (12a) and inactive constraints in Eq. (12b), the Lagrange multipliers of $Lm_p\neq 0$ and $Lm_s=0$ are discovered. Then, Y_p is a square and invertible matrix; thus, the following results are obtained, as shown in Eq. (13).

$$Y_p\omega^*-N_p=0\Rightarrow\omega^*=Y_p^{-1}N_p \tag{13}$$

It is seen from Eq. (3e) that N_p contained θ. Plugging ω^* into $f(\omega)$ of Eq. (5) yields the following optimal solution:

$$z^*(\theta) = M^T Y_p^{-1} N_p = M^T Y_p^{-1} \begin{pmatrix} b_{p_1} + \hat{F}_{p_1}^{\max} \\ H_{p_2} \hat{D} \end{pmatrix}_p = M^T Y_p^{-1} \begin{pmatrix} \begin{pmatrix} b_{p_3} + F_{p_3}^{\max} + \theta_{p_3} \\ b_{p_4} + 0 \end{pmatrix}_{p_1} \\ H_{p_2} \hat{D} \end{pmatrix}_p \tag{14}$$

$$= \left(M^T Y_p^{-1}\right)_{p_3} \theta_{p_3} + \left(M^T Y_p^{-1}\right)_{p_1} \begin{pmatrix} b_{p_3} + F_{p_3}^{\max} \\ b_{p_4} \end{pmatrix}_{p_1} + \left(M^T Y_p^{-1}\right)_{p_2} H_{p_2} \hat{D} = P\theta + w$$

where $P = \left(M^T Y_p^{-1}\right)_{p_3}$ and $w = \left(M^T Y_p^{-1}\right)_{p_1} \begin{pmatrix} b_{p_3} + F_{p_3}^{\max} \\ b_{p_4} \end{pmatrix}_{p_1} + \left(M^T Y_p^{-1}\right)_{p_2} H_{p_2} \hat{D}$.

Here, N_p is a p-dimensional row vector where $b_{p_1} + \hat{F}_{p_1}^{\max}$ are inequality constraints and $H_{p_2} \hat{D}$ are equality constraints. Where, $b_{p_3} + F_{p_3}^{\max} + \theta_{p_3}$ indicates that θ is contained by the inequality constraints and b_{p_4} does not include θ in the corresponding inequality constraints. The coefficient of θ is P and the constant term of $z^*(\theta)$ is w. As mentioned above, $\theta = \left(\theta_1\ \theta_{\dot{1}}\ \theta_2\ \theta_{\dot{2}}\ \theta_{\dot{K}}\ \theta_{\dot{K}}\right)^T_{1\times KT}$; Eq. (14) takes the following form:

$$z^*(\theta) = \left(M^T Y_p^{-1}\right)_{p_3} \theta_{p_3} + \left(M^T Y_p^{-1}\right)_{p_1} \begin{pmatrix} b_{p_3} + F_{p_3}^{\max} \\ b_{p_4} \end{pmatrix}_{p_1} + \left(M^T Y_p^{-1}\right)_{p_2} H_{p_2} \hat{D} \tag{15}$$

where the subscript of θ corresponds to the subscript of the active constraint row number A. In the same critical region, which refers to the parameter region where the optimal solution is the same, Y_p and N_p are identical. Here, θ_{p_3} refers to a row vector and $\boldsymbol{\theta}_k$ is a specific parameter.

If $\boldsymbol{\theta}_k \in \theta_{p_3}$, then the following applies:

$$\nabla_{\theta_k} z^* = \left(M^T Y_p^{-1}\right)_k^T = \left(\left(C^T\ UC^T\ SC^T\right) \begin{pmatrix} A \\ H \end{pmatrix}_p^{-1} \right)_k^T \tag{16}$$

If $\boldsymbol{\theta}_k \notin \theta_{p_3}$, then we will get the following results:

$$\nabla_{\theta_k} z^* = 0 \tag{17}$$

By evaluating the value of different variable scalar $\nabla_{\boldsymbol{\theta}_k} \bar{z}^*$ and by providing maximal social welfare with minimal investment, the transmission planners or ISOs chose which lines' capacities should be improved. Assuming the inside parameter space is set, the active and inactive constraints remained constant (i.e., in the given critical region). Therefore, parameter $\boldsymbol{\theta}_k$ is modified with the highest rate of change of the objective function z, under the effect of the parameters, because increasing the capacity of that line resulted in maximum return on investment.

Considering multiple lines' capacities can be increased simultaneously using the obtained objective function and the investment cost function regarding the increased capacity (i.e., all feasible parameter spaces), for this instance, the study finds the following optimal conditions:

$$\min\ z = F(\theta_1, \theta_2 \ldots \theta_K)$$
$$s.t. \begin{cases} IC_1(\theta_1) + IC_2(\theta_2) + \cdots + IC_k(\theta_K) \le BUD \\ 0 \le \theta_k \le \bar{\theta}_k \ \ (k = 1, 2, \ldots, K) \end{cases} \tag{18}$$

where $IC_k(\theta_K), (k = 1, 2, \ldots, K)$ represents the investment cost function for line k and $0 \le \theta_k \le \bar{\theta}_k$ denotes the potential capacity space for line K that can be increased. The largest budgetary limit for a transmission-line expansion planning project is represented by BUD. This is an optimization problem with multiple parametric variables as decision variables. The best solutions for all the uncertainty parameters are found, and we adjust the transmission capacity of each line using $(\theta_1, \theta_2 \ldots \theta_K)^*$. As a result, the lowest cost of electricity generation is achieved within the limited budget, and line congestion is reduced. This is another innovation in determining the best candidate transmission line for capacity expansion.

Based on the Simplex Method, parametric problems are solved using the optimal basic matrix, optimal solution, and optimal value. The corresponding critical region is derived using the Simplex Method because the dual solution does not depend on θ for RHS parametric linear programming problems. Two optimal basic matrices are considered as neighboring matrices when they both have optimal bases for the same θ^* in parametric space. One can transform into another via a dual step (Gal and Nedoma, 1972).

If B is an optimal basic matrix and f represents the related index set of basic variables, then Eq. (19) applies, indicating that all variables must be non-negative, which is also the primary condition of θ. This is the initial condition for the decision variables in a programming problem. The optimal decision variable results are as follows:

$$\omega^* = B_f^{-1} b(\theta) \ge 0 \tag{19}$$

At the same time, the parameters themselves have certain constraints, as shown in Eq. (20); these two sets of constraints form the range of values for the parameters under the same basic variables [50]. The feasible critical regions of the parameters are as follows:

$$G\theta \le g \tag{20}$$

To use the simplex approach, linear programming must be transformed into a standard type through slackness variables to convert all unequal constraints into equation constraints. Constraints (19) and (20) reflect the critical region. In the Lagrange method, the original inequality constraints are not normalized, and the inequality constraints contain the feasible space of the decision variables. As a result, the inactive constraint is indeterminate, and under the same active constraints and different parameters, the value on the left of the inactive constraint changes or does not satisfy the inequality relation for the inactive constraints. This indicates that the parameters are within a certain range and that the active constraints and optimal solutions are unchanged. Previous research addresses multi-parametric linear programming problems but does not describe how to construct critical regions in detail. This study uses active constraints to solve critical regions. Plug ω^* determined by Eq. (13) into inactive constraints:

$$Y_s \omega^* \le N_s \tag{21}$$

The parameter range obtained by the inequality in Eq. (21) is the feasible range of this critical region:

$$
\begin{aligned}
CR(\theta) &= \left\{ \theta \in \Theta \mid Y_s \omega^* \le N_s \right\} \\
&= \left\{ \theta \in \Theta \mid \begin{pmatrix} A \\ H \end{pmatrix}_s \begin{pmatrix} A \\ H \end{pmatrix}_p^{-1} \begin{pmatrix} \begin{pmatrix} b_{p_3} + F_{p_3}^{\max} + \theta_{p_3} \\ b_{p_4} + 0 \end{pmatrix}_{p_1} \\ H_{p_2} \hat{D} \end{pmatrix}_p \le \begin{pmatrix} \begin{pmatrix} b_{p_7} + F_{p_7}^{\max} + \theta_{p_7} \\ b_{p_8} \end{pmatrix}_{p_5} \\ H_{p_6} \hat{D} \end{pmatrix}_s \right\} \\
&= \left\{ \theta \in \Theta \mid \begin{pmatrix} A \\ H \end{pmatrix}_{p_7 \times p_3} \begin{pmatrix} A \\ H \end{pmatrix}_{p_3}^{-1} \left(b_{p_3} + F_{p_3}^{\max} + \theta_{p_3} \right) \le b_{p_7} + F_{p_7}^{\max} + \theta_{p_7} \right\} \\
&= \left\{ \theta \in \Theta \mid \theta' \le b_{p_7} + F_{p_7}^{\max} - \begin{pmatrix} A \\ H \end{pmatrix}_{p_7 \times p_3} \begin{pmatrix} A \\ H \end{pmatrix}_{p_3}^{-1} \left(b_{p_3} + F_{p_3}^{\max} \right) \right\}
\end{aligned}
\tag{22}
$$

In N_s, an *s*-dimensional row vector, there are $\begin{pmatrix} b_{p_7} + F_{p_7}^{\max} + \theta_{p_7} \\ b_{p_8} \end{pmatrix}_{p_5}$ from inequality constraints, $H_{p_6} \hat{D}$ from equality constraints, $b_{p_7} + F_{p_7}^{\max} + \theta_{p_7}$ containing Θ, and b_{p_8} without Θ from inequality constraints.

The index of the critical regions is denoted by m, where *K* refers to the set of all feasible parameters. The entire parameter space is represented by Ξ, and problems have no feasible solution in some regions, so $K \in \Xi$.

$$\bigcup CR_m = K, K \in \Xi \tag{23}$$

When the RHS of the inactive constraint $Y_s \omega^* \le N_s$ changes as a result of the parameter θ change, both active and inactive constraints are altered simultaneously, allowing this study to find new variable solutions and critical regions until the entire parameter space is covered.

If we find a new integer solution in a critical region for the relaxed LP problem, we must compare and update the upper bounds in this region before removing it from the unexplored parameter space. The mp-MILP problem is considered infeasible if the fully relaxed problem has no feasible solution. Finally, the procedure is terminated when all parameter spaces have been explored and no further solutions can be found.

4.2.2 Determine the upper bound (Step 1.2)

We use the optimal solution from the fully relaxed problem at this node to establish the upper bound within the feasible parameter space for cost-minimizing problems. This approach initiates parametric analysis for large-scale MILP, leading to an innovative and practical model.

1) To obtain the lower bound of the objective function, a relaxed mp-LP problem is solved. The critical regions *CRs* are discovered, and the optimal decision variables G and the optimal objective functions $z(\theta)$ are expressed in terms of parameters after solving the multi-parametric problem at each node.

2) Approximate integer decision variables are obtained by applying the following rule. For each binary

decision variable from the relaxed problem, if $U_m^* \geq \xi$ ($0 \leq \xi \leq 1$), we set U_m^* to one in the *m*-th critical region; otherwise, we set U_m^* to be zero. This study combines the variables U and V that emerge from this issue, and terms it UV_m. An integer linear programming (ILP) model, as shown in Eq. (24), is then constructed and solved for variable V, with fixed binary variables U.

Unlike the traditional B&B method, our approach in Eq. (24) seeks an ILP solution that meets specific conditions. Specifically, each inequality must meet the requirement that the left-hand side is less than one, and the RHS is a binary variable in the first constraint. The second inequality imposes a minimum on time limit, which must be satisfied when the corresponding binary variable U_{it} is equal to one. Similarly, the third inequality imposes a minimum off time limit, which must be satisfied when the corresponding binary variable $U_{i(t-T_i^{off})}$ is equal to zero.

Then, the optimal integer solution V is obtained:

$$\begin{aligned} &\min \quad V_{12} + V_{13} + \cdots + V_{1T} + \cdots + V_{NT} \\ &st. \begin{cases} U_{it} - U_{i(t-1)} \leq V_{it}, \ t = 2,3,\cdots,T \\ \sum_{k=t-T_i^{on}+1}^{t} V_{ik} - U_{it} \leq 0, t = T_i^{on}+1, T_i^{on}+2, \cdots, T \\ \sum_{k=t-T_i^{off}+1}^{t} V_{ik} + U_{i(t-T_i^{off})} \leq 1, t = T_i^{off}+1, T_i^{off}+2, \cdots, T \end{cases} \end{aligned} \tag{24}$$

In summary, by finding a feasible solution to the ILP problem described in Eq. (24), we can obtain the upper bound at each node for the RHS mp-MILP model in Eq. (1) based on the feasible integer solution. This approach can effectively reduce simulation time compared to the traditional B&B method.

3) When we substitute UV_m into the original MILP problem at this node in the *m*-th critical region CR_m and solve the LP problem in region CR_m. The corresponding updated optimal decision variable $\bar{G}_m$ is found, and the sub-region upper objective function $\bar{z}_i(\theta)$ with parameters θ in the CR_m is denoted.

4) At node *i*, the problem's upper bound $\bar{z}_i(\theta)$ is obtained by combining the sub-region upper bound objective functions $\bar{z}_{i,m}(\theta)$ across all regions $CR_{i,m}$.

4.2.3 Compare the objective function of the current solution with the current upper bound (Step 1.3)

The lower bound for the original problem is determined at the root node. Meanwhile, the upper bound $\bar{z}_i(\theta)$ established at the root node in Section 4.2.2 serves as the initial upper bound $\bar{z}(\theta)$ for the problem.

At each node *i*, the objective value $\hat{z}_i(\theta)$—which is the lower bound—is calculated by relaxing the problem, along with the associated upper bound $\bar{z}(\theta)$, across all parameter regions. To simplify the analysis, we select Q random points within the parameter. The errors between the upper and lower bounds at each point are calculated. These errors are then used to compute the final error rate by applying a weighted average across all selected random points, as detailed in Eq. (25).

$$\delta = \left(\sum_{j=1}^{Q} \frac{\bar{z}(\theta) - \hat{z}_i(\theta)}{\hat{z}_i(\theta)} \right) \Big/ Q \tag{25}$$

If the error rate $\delta \le \alpha$, the calculation process concludes; otherwise, the procedure advances to Step 2. Here, α represents a hypothetical threshold or error-tolerance limit, adjustable to align with real market objectives or computational burdens—an innovative aspect of this study.

4.3 Select a branching variable and update the set of nodes N (Step 2)

A binary variable from vector U is selected, and two new node-fixing variables are generated, each set to 0 and 1, respectively. The unexplored parameter spaces of these nodes, Ξ_{n+1} and Ξ_{n+2}, correspond to the remaining critical regions. We then add the new nodes to N and $n = n + 2$ is updated (i.e., we add two nodes to each branch).

4.4. Determine at the node (Step 3)

If $N = \{\varnothing\}$, no solutions are found, the iteration stops; otherwise, we select a node i from N and remove it from the list of uncalculated nodes: $n = n - 1$. Here, n is the number of nodes that are not yet calculated.

4.5. Solve and compare (Step 4)

By substituting fixed binary variables into the mp-LP problem (referring to Eq. (2) in the first iteration and Eq. (26) in next subsequent iteration), Eq. (26) is obtained. Here, ω' denotes the variable vector after the binary variables are determined by substitution:

$$\begin{aligned} &\hat{z}(\theta) = \min_{G,U,V} M^T \omega' \\ &st. \begin{cases} A\omega' \le b + \hat{F}^{\max} \\ H\omega' = H\hat{D} \end{cases} \end{aligned} \tag{26}$$

The mp-LP problem is solved for node i with unknown parameter spaces Ξ_i, using the Lagrange method as Step 1. If the problem is infeasible for all $\theta \in \Xi_i$, we must go back to step 3. On the other hand, if the problem is feasible, we determine and update the upper bound as in Step 1; the upper bound obtained at node i is recorded as $\bar{z}_i(\theta)$. The $\bar{z}_i(\theta)$ and current upper bound $\bar{z}_{old}(\theta)$ are segmented by piecewise functions over the region. Here, $\bar{z}_{old}(\theta)$ refers to the optimal global upper bound as the algorithm progresses to node i. This study merges critical regions of $\bar{z}_i(\theta)$ and $\bar{z}_{old}(\theta)$ to generate new critical regions and selects a smaller upper bound $\bar{z}_i(\theta)$ and $\bar{z}_{old}(\theta)$. In every new critical region, we select the smaller upper bound $\bar{z}_{new}(\theta)$ across all parameter regions (Dua and Pistikopoulos, 2000). Decision-makers calculate the error between the optimal function value $\hat{z}_i(\theta)$ at node i and the current upper bound $\bar{z}_i(\theta)$; if $\delta \le \alpha$ holds, the iteration ends; otherwise, we continue.

This study compares the solution at node i with the current upper bound, $\bar{z}_{old}(\theta)$. The obtained optimal

solution for the transmission planning problem at node *i,* denoted as $\hat{z}_i(\theta)$, and it is composed by *m* optimal value linear functions $\hat{z}_{i,m}(\theta)$. The corresponding critical region is identified as $CR_{i,m}$. The current upper bound is recorded as $\bar{z}_{old}(\theta)$ and is defined by a set of functions, $\bar{z}_{m'}(\theta)$, and their corresponding critical regions are $CR_{m'}^{UB}$. Their intersection is shown in CR^{int} in Eq. (27):

$$CR^{\text{int}} = CR_{i,m} \cap CR_{m'}^{UB} \tag{27}$$

If $CR^{\text{int}} \neq \varnothing$ and the optimal solution is greater than the upper bound in the m-th critical region, it should be removed from the uncertain space. One must check whether $\hat{z}_{i,m}(\theta)$ is smaller than $\bar{z}_{m'}(\theta)$:

$$\hat{z}_{i,m}(\theta) - \bar{z}_{m'}(\theta) \leq 0 \tag{28}$$

4.6. Determine nodes and critical region of θ (Step 5)

If any of the following conditions are met within a certain parameter space, that space is removed from Ξ_i, indicating it is part of the Sensitivity parameter space at node *i*:

(i) The problem is not feasible.

(ii) A better integer solution is found.

(iii) The solution of a node is greater than the current best upper bound in the same space.

This process simplifies the operational steps and facilitates iteration through all nodes in all parameter spaces. If the values of all binary variables U at node *i* are fixed, planners update the upper bound by employing the comparison method outlined in Step 4. If all the critical regions of node *i* are eliminated, we return to Step 3 to explore the uncalculated node; otherwise, we return to Step 2 to build a new branch.

In summary, considering transmission capacity constraints, generation and demand-balance conditions, physical constraints of generators, and the ongoing increase in the demand for renewable energy, this research develops a RHS mp-MILP model to reflect the uncertainty in line capacity. The steps outlined in Section 4 yield the following managerial insight and application.

Managerial Insight and Application: *Parametric analysis enables the identification of congestion in specific lines based solely on function parameters and facilitates the establishment of a mathematical relationship between system costs and line capacity expansions. By analyzing the marginal benefits, such as decrease in system costs from increased line capacity versus the costs of upgrading line capacity, transmission line planners can effectively implement suitable line-capacity enhancements. This approach enables them to allocate resources efficiently and maximize social welfare with minimal investment.*

5. Case Study

We validate the proposed methodologies and results in Section 5.1 using a single-period SCUCED case to illustrate the calculation procedure in detail, which has two buses and two parameters, each representing the increased capacity of a transmission line. In Section 5.2, we employ the IEEE 5-bus SCUCED case with

24 periods to demonstrate the results and insights. For simplicity, we consider only one line's capacity uncertainty. Section 5.2 builds upon the previous explanation by applying our approach to an IEEE 5-bus SCUCED with multiple periods that involves 335 binary decision variables. Despite the complexity, our approach successfully manages this large number of variables, highlighting its robustness and efficiency. It is noteworthy that existing tools for parametric analysis in MILP typically support only up to 50 integer variables. In Section 5.3, we extend our analysis to the IEEE 30-bus case, which incorporates 720 integer variables. This case further demonstrates the scalability of our approach, illustrating its effectiveness in managing a more complex system. The inclusion of this case study highlights our methodology's ability to perform effectively across various scenarios, from those with only 2 binary variables in Section 5.1 to those with 335 and 720 binary variables in Sections 5.2 and 5.3, respectively.

5.1 Single Period Synthetic Case

Consider the following example of MILP parametric analysis, where $D_1(7)+D_2(8)$ indicates that the demand at bus 1 and 2 are 7 and 8 units, respectively:

$$
\begin{aligned}
& z(\theta) = \min_{x,y} 3x_1 + 5x_2 + 18y_1 + 15y_2 \\
& s.t. \quad \begin{cases} x_1 + x_2 = 15 = D_1(7) + D_2(8) \\ 0.8x_1 + 0.7x_2 \le 11.2 + \theta_1 \\ 0.6x_1 + 0.9x_2 \le 12.4 + \theta_2 \\ x_1 - 10y_1 \le 0 \\ x_2 - 10y_2 \le 0 \\ y_i \in \{0,1\}, i = 1,\ 2;\ 0 \le \theta_s \le 10,\ s = 1,\ 2;\ x_j \ge 0,\ j = 1,\ 2 \end{cases}
\end{aligned} \tag{29}
$$

In this single-period problem, the constraints for the start-up ramp rate, shut-down ramp rate, and the relationship between the UC of generators and the start-up state are ignored. This removal also eliminates the contrasts for minimum on time and minimum off time. Only the energy balance and generation constraints are considered. In this synthetic case, two generators and two buses are connected by two lines. This case study incorporates two uncertainty parameters on the RHS of the transmission lines' capacity constraints, demonstrating the proposed methods from Section 4 and illustrating the lines' capacity uncertainty. Both parameters range from 0 to 10, indicating potential enhancements in line capacities within this range. Because there are few integer variables, for simplicity, the upper bound at each node is not considered in this case (see Appendix B for derivations). Instead, we demonstrate how to compute the critical region. This problem will be solved based on the following steps:

Step 0: Initialize the collection of nodes that need to be solved: denoted as $N = \{\varnothing\}$ and set the node counter $n = 0$.

Step 1: Solve the fully relaxed problem as follows (at node 0):

$$z(\theta) = \min_{x,y} 3x_1 + 5x_2 + 18y_1 + 15y_2$$

$$s.t. \begin{cases} x_1 + x_2 = 15 = D_1(7) + D_2(8) \\ 0.8x_1 + 0.7x_2 \le 11.2 + \theta_1 \\ 0.6x_1 + 0.9x_2 \le 12.4 + \theta_2 \\ x_1 - 10y_1 \le 0 \\ x_2 - 10y_2 \le 0 \\ -y_1 \le 0 \\ -y_2 \le 0 \\ y_1 \le 1 \\ y_2 \le 1 \\ 0 \le \theta_s \le 10,\ s = 1, 2;\ x_n \ge 0,\ n = 1, 2 \end{cases} \tag{30}$$

Based on the steps introduced in Section 4, when $\theta_1 = 0$ *and* $\theta_2 = 0$, using Eq. (13) in Section 4, the best decision variable, $\omega_{0,1}^*$, as shown in Eq. (7b), is derived as follows:

$$\omega_{0,1}^* = A_p^{-1}(b_p + F_p^{\max} + \theta_p) = \begin{pmatrix} 10 \cdot \theta_1 + 7 \\ 8 - 10 \cdot \theta_1 \\ \theta_1 + 7/10 \\ 4/5 - \theta_1 \end{pmatrix} \tag{31}$$

Based on Eq. (22), the critical region is as follows:

$$CR_{0,1} = \left\{ \theta \in \Theta \mid A_s \omega^* \le b_s + \hat{F}_s^{\max} \right\} = \left\{ 0 \le \theta_1 \le 0.3, 0 \le \theta_2 \le 10 \right\} \tag{32}$$

The optimal objective function at the root node is:

$$z_{0,1} = 85.6 - 17.0 \cdot \theta_1, when \left\{ 0 \le \theta_1 \le 0.3, 0 \le \theta_2 \le 10 \right\} \tag{33}$$

Here, θ is recognized as a decision variable and is then used to calculate the first-order response function of $z_{0,1} = 85.6 - 17 \cdot \theta_1$ on θ using Eq. (17). We then determined the cost reduction rate (i.e., the first-order derivative) with the upgrade of the transmission line's capacity in the same critical region (e.g., $\left\{ 0 \le \theta_1 \le 0.3, 0 \le \theta_2 \le 10 \right\}$).

Here, S indicates the set of active constraints from *A*. From Eq. (7b), the following results are obtained.

$$S = \left\{ S_1, S_2, S_3 \right\} = \left\{ 1, 5, 6 \right\} \tag{34}$$

Here, S' denotes the inequality constraint row subscripts with the parameters on the RHS.

$$S' = \left\{ S_i \mid S_i \in \left\{ 1, 2 \right\} \right\} \tag{35}$$

For the first parameter θ_1, since $S_1 = 1 \in S'$, we have:

$$\nabla_{\theta_1}\overline{z}^* = \left(\begin{pmatrix} A_{p-1} \\ H \end{pmatrix}^{-1}\right)_1^T \cdot \left(C^T \; SC^T\right)^T = -17, S_1 \in S' \tag{36}$$

For the second parameter θ_2, because $\forall\ S_i \notin S'$, we have:

$$\nabla_{\theta_2}\overline{z}^* = \mathbf{0} \tag{37}$$

The results from Eqs. (36) and (37) reveal that increasing the capacity of the first line by one unit reduces the cost of electricity generation by 17 units; however, increasing the capacity of the second line does not affect system costs. Therefore, increasing the capacity of the second line does not benefit ISO's optimization goal.

When the parameter $\theta_1 = 0.3$, the fourth constraint, initially inactive in the matrix A_s from Eq. (8b), becomes active. Conversely, the first active constraint in the matrix A_p from Eq. (7b) becomes inactive, thereby altering the matrix A_p in Eq. (7b). Similarly, using Eqs. (13), (14), and (22), the best expression for the decision variables $\omega_{0,2}^*$, the critical region $CR_{0,2}$, and the optimal objective function $z_{0,2}^*$ are calculated. The method for determining the analytically best objective function and related critical regions by utilizing active and inactive constraints is determined using optimal Lagrange multipliers.

$$\omega_{0,2}^* = A_p^{-1}(b_p + F_p^{\max} + \theta_p) = \left(10 \;\; 5 \;\; 1 \;\; 0.5\right)^T \tag{38}$$

$$CR_{0,2} = \left\{\theta \in \Theta \mid A_s\omega^* \le b_s + \hat{F}_s^{\max}\right\} = \left\{0.3 \le \theta_1 \le 10, 0 \le \theta_2 \le 10\right\} \tag{39}$$

$$z_{0,2}^* = 80.5, when\ \left\{0.3 \le \theta_1 \le 10, 0 \le \theta_2 \le 10\right\} \tag{40}$$

In this critical region (i.e., $0.3 \le \theta_1 \le 10, 0 \le \theta_2 \le 10$), this study explores the impact of changes in transmission line capacity on system costs, specifically examining the effects on the optimal objective function. Here, S is determined using Eq. (7b) and S' is the same as in Eq. (35).

$$S = \{S_1, S_2, S_3\} = \{5, 6, 7\} \tag{41}$$

For the first parameter, θ_1, and the second parameter, θ_2, because $\forall\ S_i \notin S'$, the calculation is:

$$\nabla_{\theta_1}\overline{z}^* = \mathbf{0} \tag{42}$$

$$\nabla_{\theta_2}\overline{z}^* = \mathbf{0} \tag{43}$$

The findings from Eqs. (42) and (43) indicate that increasing the capacity of the first and second lines has no effect on the optimal electricity generation cost outcome $\overline{z}^*$ within the second critical region (i.e., $0.3 \le \theta_1 \le 10, 0 \le \theta_2 \le 10$). We acknowledge that this is our innovation in identifying which lines' capacity to upgrade its capacity and to what extent, from the perspective of the ISO, to minimize the system cost.

Step 2: Choose a node and fix UC binary variables, either $y_1 = 0$ or $y_1 = 1$. Set the unexplored parameter space of these nodes as Ξ_1 and Ξ_2, respectively. Update the node count to $n = 2$ and $N = \{y_1 = 0, y_1 = 1\}$.

Step 3: Fix $y_1 = 0$, and $n = 1$, $N = \{y_1 = 1\}$.

Step 4: ***Node1*** (Fix $y_1 = 0$): The problem is infeasible; therefore, this node is fathomed.

Step 5: Return to **Step 3** due to $\Xi_1 = \varnothing$.

Step 3: Fix $y_1 = 1$, and $n = 0$, $N = \varnothing$.

Step 4: ***Node2*** (Fix $y_1 = 1$): The problem is feasible.

According to the Lagrange method, the optimal function/value is determined using Eq. (13), the critical region is based on Eq. (14), and the optimal decision variable could be obtained from (22). The optimal solutions are shown as follows:

$$\begin{cases} x_1 = 10 \cdot \theta_1 + 7, x_2 = 8 - 10 \cdot \theta_1, y_1 = 1, y_2 = 0.8 - \theta_1 \\ z_{2,1}(\theta) = 91.0 - 35 \cdot \theta_1 \qquad CR_{2,1} = \{\Theta \mid 0 \le \theta_1 \le 0.3, 0 \le \theta_2 \le 10\} \\ x_1 = 10, x_2 = 5, y_1 = 1, y_2 = 0.5 \\ z_{2,2}(\theta) = 80.5 \qquad CR_{2,2} = \{\Theta \mid 0.3 \le \theta_1 \le 10, 0 \le \theta_2 \le 10\} \end{cases} \tag{44}$$

Step 5: Return to **Step 2** due to $\Xi_2 = \{\Theta \mid 0 \le \theta_1 \le 10, 0 \le \theta_2 \le 10\}$.

Step 2: Choose a node and fix the *UC* (i.e., binary variables), $y_2 = 0$ or $y_2 = 1$. Define the unexplored parameter spaces for these nodes as Ξ_1 and Ξ_2 ,respectively. Update the node count $n = 2$ and $N = \{y_1 = 1, y_2 = 0; y_1 = 1, y_2 = 1\}$ adjust accordingly.

Step 3: Fix $y_1 = 1, y_2 = 0$, and $n = 1$, $N = \{y_1 = 1, y_2 = 1\}$.

Step 4: ***Node3*** (Fix $y_1 = 1, y_2 = 0$): The problem is infeasible.

Step 5: Return to **Step 3** due to $\Xi_1 = \varnothing$.

Step 3: Fix $y_1 = 1, y_2 = 1$, and $n = 0$, $N = \varnothing$.

Step 4: ***Node4*** (Fix $y_1 = 1, y_2 = 1$): Node 4 is plugged into the original problem, and the updated optimization problem is obtained. Similarly, using Eqs. (13) and (14), the optimal solutions (e.g., optimal decision variables, optimal objective functions, and corresponding critical regions) are

$$\begin{cases} x_1 = 10 \cdot \theta_1 + 7, x_2 = 8 - 10 \cdot \theta_1, y_1 = 1, y_2 = 1 \\ z_{4,1}(\theta) = 94.0 - 20.0 \cdot \theta_1 \qquad CR_{4,1} = \{\Theta \mid 0 \le \theta_1 \le 0.3, 0 \le \theta_2 \le 10\} \\ x_1 = 10, x_2 = 5, y_1 = 1, y_2 = 1 \\ z_{4,2}(\theta) = 88.0 \qquad CR_{4,2} = \{\Theta \mid 0.3 \le \theta_1 \le 10, 0 \le \theta_2 \le 10\} \end{cases} \tag{45}$$

Based on the results of Eq. (45), the transmission planners should increase the 0.3-unit capacity of the first line. The results of Eq. (45) show that 1) increasing the capacity of the second line had no effect on the

reduction of system costs, indicating that this line is not congested in the original problem; and 2) in the same situation, increasing the capacity of the first line by more than 0.3-unit capacity had no effect on the optimization results.

Step 5: Return to **Step 3** due to $\Xi_2 = \varnothing$.

Step 3: Since $N = \{\varnothing\}$, the iteration with solutions must be stopped.

In summary, this study drew the following optimal three-dimensional plane curve through multi-parametric toolbox (MPT) (see https://www.mpt3.org/Main/HomePage for details).

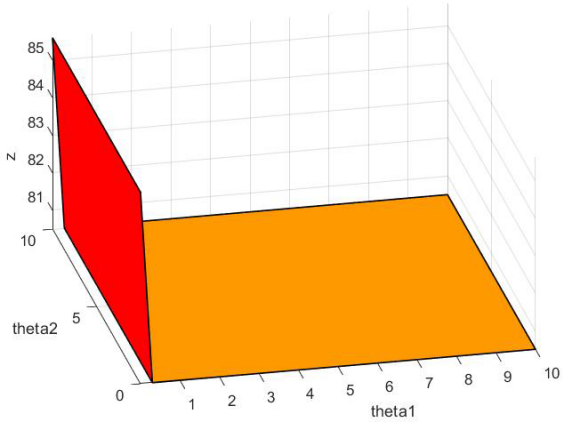

Fig. 2: Optimal solution with parametric analysis (at node 0)

$$\begin{cases} z_1 = 85.6 - 17.0 \times \theta_1, where,\ 0 \le \theta_1 \le 0.3, 0 \le \theta_2 \le 10 \\ z_2 = 80.5, where,\ 0.3 \le \theta_1 \le 10, 0 \le \theta_2 \le 10 \end{cases}$$

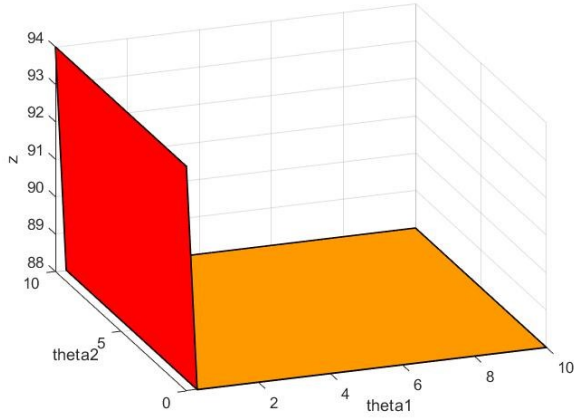

Fig. 3: Optimal solution with parametric analysis (at node 4)

$$\begin{cases} z_1 = 94.0 - 20.0 \times \theta_1, where,\ 0 \le \theta_1 \le 0.3, 0 \le \theta_2 \le 10 \\ z_2 = 88.0, where,\ 0.3 \le \theta_1 \le 10, 0 \le \theta_2 \le 10 \end{cases}$$

Figure 2 displays the exact optimal parametric analysis solution, which considers the capacity uncertainties of two transmission lines at the root node, achieved by relaxing all binary variables to continuous ones. This is a three-dimensional plane, with three dimensions representing theta1, theta2, and z. A lower bound of the mp-MILP problem is presented in this figure. According to the previous calculation process, the global optimal solution to the mp-MILP problem that satisfies all constraints is obtained at node 4 and the calculation ends. Two parameter regions and the corresponding optimal objective function expression are obtained. Figure 3 depicts the relationship between the parameters (θ_1, θ_2) and the ideal objective function value at node 4 (i.e., $y_1 = 1$ and $y_2 = 1$). This constitutes the final, optimal solution for the mp-MILP problem as per Eq. (29), satisfying all constraints.

Unlike traditional B&B methods, which typically focus on solving either the upper or lower bounds at each branching point, our approach concurrently resolves both bounds while integrating a tolerance range for acceptable errors. This enhancement not only accelerates the convergence process but also significantly improves the efficiency of the iteration cycle. By implementing a tolerance range, our method effectively balances computational accuracy with processing speed, providing a robust solution framework that is especially beneficial in large-scale optimization scenarios. These scenarios often challenge traditional B&B methods due to their computational intensity and the complexity of the problems involved. Our novel approach not only expedites the solution process but also extends the scalability and applicability of the

B&B method to more complex mp-MILP problems, which are increasingly prevalent in modern industrial and systems engineering applications.

5.2 IEEE 5-bus case with 24-periods SCUCED

This section demonstrates the application of the proposed method to a 24-period IEEE-5 bus SCUCED problem. This problem has five buses and six lines, and all data (i.e., transmission capacity, generation shift factor, and per-unit electricity generation cost) are extracted in MATLAB using MATPOWER. The total load profile was sourced from the University of Washington's database (available at https://labs.ece.uw.edu/pstca/rts/pg_tcarts.htm). The load was then distributed among the three buses (B, C, and D) in the ratios of 30%, 30%, and 40%, respectively. To simplify and intuitively demonstrate the algorithm and conclusion, we only consider the uncertainty of the transmission capacity of line 4 in this section (i.e., parametric analysis for other line capacity upgrading, see Appendix C).

As a result, this algorithm derives the lower bound $\underline{z}_4$ in the entire parameter space by solving the fully relaxed problem because the variables range of the mp-MILP problem is a subset of that for the fully relaxed problem. Solving the mp-LP problem yields a lower bound for the mp-MILP problem by treating the binary variables as continuous variables between 0 and 1.

$$\underline{z}_4 = \begin{cases} 417617.46 - 90.603117 \cdot \theta_4, \ 0 \le \theta_4 \le 6.453 \\ 417375.54 - 53.113796 \cdot \theta_4, \ 6.453 \le \theta_4 \le 14.935 \\ 417352.34 - 51.553703 \cdot \theta_4, \ 14.935 \le \theta_4 \le 15.857 \\ 417079.85 - 34.369136 \cdot \theta_4, \ 15.857 \le \theta_4 \le 21.170 \\ 416352.25, \ 21.170 \le \theta_4 \le 100 \end{cases} \tag{46}$$

The parameter space is divided into five critical regions, each with an optimal parametric analysis objective function represented as a piecewise affine function split into five segments. Eq. (47) reveals that the optimal objective function is a constant value when $44.2195 \le \theta_4 \le 100$. Here, we use subscript *k* to emphasize the dependence of the optimal solution on which the line's capacity was upgraded.

After obtaining the fully relaxed solution at the root node, Eq. (24) is employed, and the obtained optimal continuous variables are transformed to zero or one. Here, assuming $\xi = 0$ (the UC variables), then fixing these variables, the upper bound of the IEEE-5 bus SCUCED problem is discovered by solving the mp-LP problem after converting continuous variables to binary variables.

$$\overline{z}_4 = \begin{cases} 417635.23 - 90.580071 \cdot \theta_4, \ 0 \le \theta_4 \le 6.453 \\ 417389.37 - 53.100241 \cdot \theta_4, \ 6.453 \le \theta_4 \le 14.935 \\ 417366.17 - 51.540488 \cdot \theta_4, \ 14.935 \le \theta_4 \le 15.857 \\ 417091.76 - 34.360325 \cdot \theta_4, \ 15.857 \le \theta_4 \le 21.170 \\ 416364.35, \ 21.170 \le \theta_4 \le 100 \end{cases} \tag{47}$$

The error values in each critical region between $\underline{z}_4$ and $\overline{z}^4$ are calculated when the upper and lower bounds at the root node are obtained. Here, we assume that $\alpha = 0.01$ corresponds to the actual situation and represents the upper bound of the transmission planner's tolerance error, which is calculated using Eq. (25). In this case, we compute the error by randomly selecting 50 values (i.e., $Q = 50$) from each critical region.

$$\delta_4 = \begin{cases} 0.00425\%, & 0 \le \theta_4 \le 6.453 \\ 0.03359\%, & 6.453 \le \theta_4 \le 14.935 \\ 0.00336\%, & 14.935 \le \theta_4 \le 15.857 \\ 0.00285\%, & 15.857 \le \theta_4 \le 21.17 \\ 0.00291\%, & 21.17 \le \theta_4 \le 100 \end{cases} \tag{48}$$

The error in each crucial zone is less than 0.034%, which is within the permitted range (i.e., $\delta < \alpha = 0.01$), so the iteration operation is terminated, as specified in Step 1 of Section 4. Compared with traditional B&B methods for exploring all potential nodes, this study concludes that the approximate optimal solution to this problem is obtained quickly based on the proposed method.

Furthermore, the accuracy of the approximation is notably high, at approximately 99.994% for this problem. Therefore, by using the improved B&B method, the final optimal approximate results are obtained, which is the upper bound curve in Figure 4.

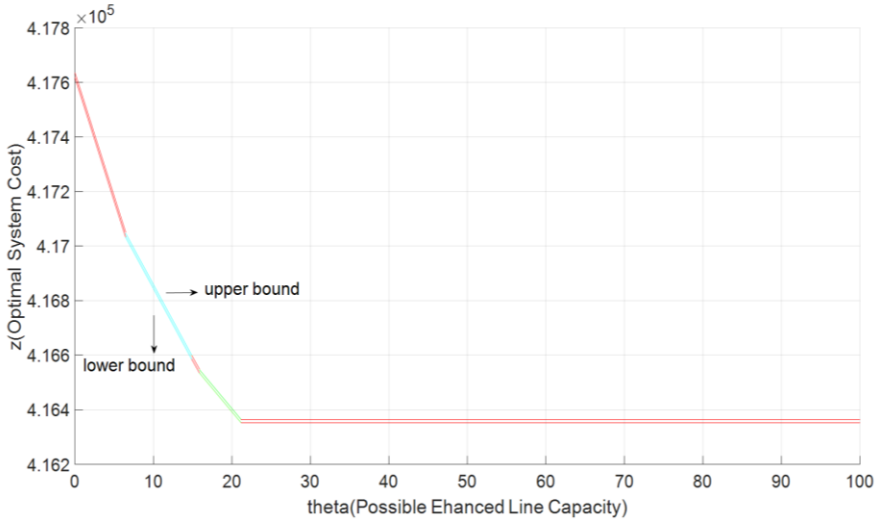

Fig. 4: The lower and upper boundaries at root node when upgrading the capacity of line 4

The horizontal axis of the graph indicates the range of the parameter theta or the possible space for increasing the transmission line capacity, and the vertical axis represents the best objective value (i.e., system costs). The difference between the lower and upper bound curves represents the error in Eq. (48). The optimal solution falls within the lower and upper bound curves in Figure 4, which indicates the benefit of increasing line 4's capacity over 24 hours.

However, when we use the MPT solver in MATLAB, the traditional B&B method is not supported due to the large number of binary values and the massive number of possible nodes. The SCUCED example in this IEEE 5-bus 24-period case contains a total of 335 binary decision variables. This includes 120 binary decision variables for the 24 UC periods across 5 buses (24 * 5 = 120) and 115 binary decision variables representing the UC start state, calculated as $(T-1)\times N$ (where T=24 and N=5, leading to 23×5=115). According to our test, the MPT can only handle roughly 50 binary variables if we employ the traditional B&B method. As a result, we can reasonably conclude that the proposed approach in this study, which

employs the parametric analysis method, can address large systems planning problems more effectively than the traditional B&B method, particularly when there are more binary variables.

For the IEEE 5-bus with a 24-period SCUCED case, the current capacity of Line 4 is 150 MW. The first line segment (first critical region) in Eq. (48) shows that increasing line 4's capacity from 150 MW up to 156.453 MW results in a system cost reduction of $90.580071 for each additional MW. This also implies that the optimal action to take for the transmission planner is to increase the capacity of line 4 up to 156.453 MW (i.e., 150+6.453) to reduce generation costs, if and only if the cost of the unit capacity of the line upgrade is lower than $90.580071. Therefore, the ISO should abandon the strategy of upgrading line 4's capacity to lower generation costs if the marginal cost per unit capacity of line 4 is higher than $90.580071.

The second line segment (third critical region) indicates that increasing line 4's capacity from 156.453MW (i.e., 150+6.453) to 164.935 MW (i.e., 150+14.935) results in a system cost reduction of $53.100241 for each additional MW. Therefore, from the first two critical regions, we can conclude that the planner should increase line 4's capacity up to 164.935mw in order to minimize the generation cost if the cost of the unit capacity of the line upgrade is lower than $ 53.100241. The fifth line demonstrates that increasing the capacity of line 4 does not benefit the system if the existing capacity is already more than 171.170 MW (i.e., 150+21.170=171.170).

Therefore, utilizing the approximated optimal solution in equation (48) and Figure 4, the relationship between the optimal capacity upgrade for line 4 and the marginal cost of the capacity of the line 4 upgrade is plotted in Figure 5. Using the findings of the previous study (Baldick and Neill, 2009), we calculated the line 4 upgrade cost, which is a one-time investment cost. Simply multiplying the 24-hour benefit from equation (47) by 365 yields the annual benefit. Next, we compare the cost of the capacity upgrade with the annual benefit.

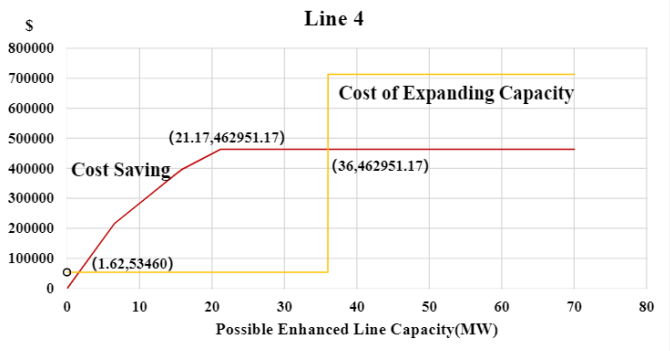

Fig. 5: The optimal suitable amount of capacity upgrade for line 4

Figure 5 demonstrates how to select the optimal amount of capacity upgrade by balancing the cost reduction rate of the objective function on the parameters with the cost per unit capacity of the line upgrade, thereby reducing system generation costs. As a result, transmission planners or the ISO must balance the marginal benefits of increased line capacity against the cost of improving line capacity. Although system costs decrease as line capacity increases, the marginal benefit of each additional unit of capacity diminishes.

5.3 IEEE 30-bus Case with 24-periods SCUC/SCED

This section demonstrates the application of the proposed method to a 24-period IEEE 30-bus SCUC/SCED problem. The system includes 30 buses, 41 transmission lines, and 6 generators, with all relevant data (i.e., transmission capacities, generation shift factors, and per-unit electricity generation costs) extracted in MATLAB using MATPOWER. The total load profile was derived from the CAISO daily load trend (available at https://www.caiso.com/todays-outlook) and the IEEE 30-bus case data (available at https://matpower.org/docs/ref/matpower5.0/case_ieee30.html). The load was then distributed among the buses in proportions that reflect typical operational scenarios.

To increase the complexity to our analysis, we extended the original IEEE 5-bus case by implementing a parametric analysis of the UCED problem on the IEEE 30-bus system. This involved introducing 24 virtual generators (each with $Gmax = Gmin = 0$) and zero generation cost to maintain the model's structure. Since the IEEE 30-bus case provides single-period load data, we created a realistic load profile for 24 periods using the CAISO daily load trend, scaling it to match the total generation capacity of the six generators. Additionally, we introduced fixed costs for turning on each generator, proportional to $Gmax$, while assuming zero start-up costs for simplicity. Notably, the impact of the UC start state was ignored, calculated as $(T-1)\times N$ (where T=24 and N=30, leading to 23×30=690). Thus, the total number of binary decision variables included 720 for the 24- UC periods across 30 buses (24 * 30 = 720).

To streamline the analysis, we focused on the uncertainty of transmission line 15's capacity. The algorithm derives the lower bound in the entire parameter space by solving the fully relaxed problem, as the variable range of the mp-MILP problem is a subset of that for the fully relaxed problem. Solving the mp-LP problem yields a lower bound for the mp-MILP problem by treating the binary variables as continuous variables between 0 and 1.

After obtaining the fully relaxed solution at the root node, we transformed the optimal continuous variables into binary variables. This transformation allows us to discover the upper bound of the IEEE 30-bus SCUCED problem by solving the mp-LP problem after fixing these variables. The parameter space is divided into three critical regions, each defined by the operational limits of transmission line 15. We evaluated the performance of the proposed method by computing the error values in each critical region. The errors were calculated using 50 randomly selected values from each region, resulting in the following average error values: Region 1 exhibited an average error of approximately 0.0085%, while Region 2 and Region 3 both showed an average error of 0.0%. The overall average error across all regions is approximately 0.00282%, leading to an overall accuracy of approximately 99.9972%. Consequently, we derived the approximate optimal solution using the upper boundary determined, as follows:

$$\bar{z}_{15} = \begin{cases} 272086.62 - 34.360325 \cdot \theta_{15}, \ 0 \le \theta_{15} \le 3.64 \\ 272001.05 - 17.171093 \cdot \theta_{15}, \ 3.64 \le \theta_{15} \le 29.31 \\ 271497.84, \ 29.31 \le \theta_{15} \le 100 \end{cases} \tag{49}$$

These results demonstrate the efficiency in convergence and accuracy of our approach, especially when compared to traditional branch-and-bound (B&B) methods, which often struggle with the high number of binary decision variables involved. The optimal approximate results are illustrated in the upper bound curve shown in Figure 6.

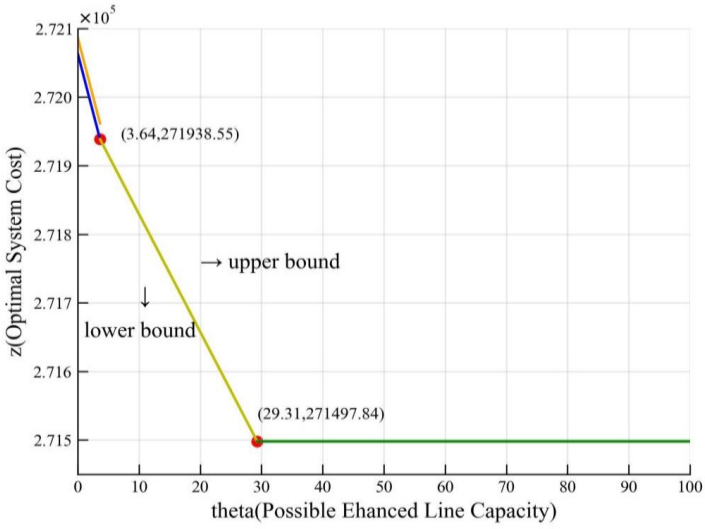

Fig. 6: The lower and upper boundaries at root node when upgrading the capacity of line 15

The horizontal axis of the graph indicates the parameter space for θ_{15}, while the vertical axis represents the best objective value (i.e., system costs) in Figure 6. The difference between the lower- and upper-bound curves illustrates the operational cost implications of capacity upgrades for line 15 across different load scenarios. Utilizing the approximated optimal solution in Eq. (49) and the data from Figure 6, the relationship between the optimal capacity upgrade for line 15 and the marginal cost of the upgrade is plotted in Figure 7.

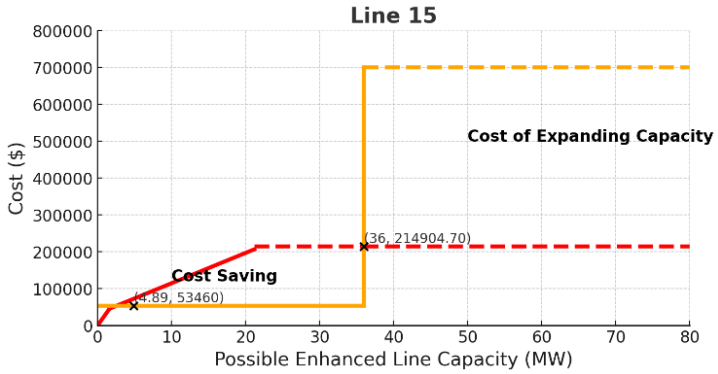

Fig. 7: The optimal suitable amount of capacity upgrade for line 15

Figure 7 presents similar results to those observed in Figure 5, illustrating the relationship between capacity upgrades and the corresponding reductions in system costs. The marginal cost of the capacity upgrade for line 15 follows a trend similar to that seen for line 4, demonstrating consistent operational cost

savings as capacity is enhanced. Moreover, the calculation method for capacity investment costs is identical for both line 15 and line 4. As outlined in Section 5.2 and based on Baldick and Neill (2009), we treat the upgrade cost as a one-time investment. By multiplying the 24-hour benefit from Equation (47) by 365, we derive the annual benefit, enabling a direct comparison between the upgrade costs and the projected annual savings for each line. This consistent methodology ensures the comparability of results across different lines within the system.

In our study, we utilized a variety of computational tools within MATLAB to address the challenges posed by mp-MILP problems. General solvers such as linprog, quadprog, and fmincon were employed, alongside commercial solvers like CPLEX and Gurobi. However, it's important to note that CPLEX and Gurobi currently do not support solving mp-MILP problems directly. More information can be found on their respective websites: CPLEX Optimizer (https://www.ibm.com/products/ilog-cplex-optimization-studio/cplex-optimizer/) and Gurobi Optimizer (https://www.gurobi.com/solutions/gurobi-optimizer/). This limitation necessitates alternative solutions for handling complex parameter interactions and deriving analytical solutions within each parameter region.

The advantage of using mp-MILP lies in its ability to generate optimal function expressions specific to each parameter region, offering nuanced insights for decision-making beyond the capabilities of methods that yield a single optimal outcome. For instance, our approach effectively managed a scenario involving 720 integer variables—significantly more than the 50 integer variables limit of the MPT3 solver (see https://www.mpt3.org/), which frequently times out beyond this threshold. To expedite convergence and achieve this result, we applied a strategic value assignment where variables with relaxed values exactly equal to zero were set to zero, and those with relaxed values between zero and one were set to one. This method of fixing variables based on relaxed problem results, determined through extensive testing to be the most effective for rapid convergence, helped us quickly reduce the computational space and accelerate the solving process. As a result, we obtained an analytically approximate optimal solution for mp-MILP. The precision of this solution was remarkably high, achieving an accuracy of approximately 99.994% in the IEEE 5-bus case and 99.9972% in the IEEE 30-bus case.

This performance was facilitated by the computational power of a 16-core AMD Ryzen 9 3950X CPU at 3.49 GHz with 64 GB of RAM, using MATLAB R2023a and Yalmip 2023. We obtained an approximate optimal solution in 49,387.33 seconds (equivalent to 13 hours and 43 minutes) for the IEEE-30 bus case, and 2,361.61 seconds (equivalent to 39 minutes) for the IEEE 5-bus case. Compared to related studies, such as those by Charitopoulos et al. [37], who handled up to 25 integer variables, and Oberdieck et al. [74], who dealt with up to 10 optimization variables and 240 constraints, our study demonstrates significant advancements in tackling larger scale problems more efficiently and effectively.

Our method allows us to obtain upper bounds at each node, which reduces the number of nodes that need to be searched for solutions. In contrast to the B&B method that aims to find the optimal solution, our approach provides a feasible solution within a tolerance range of error. The use of upper bounds obtained by our method can guide the search for an optimal solution, allowing the B&B algorithm to focus on

promising nodes and further reducing computation time. Overall, our approach offers a practical solution for solving MILP problems, providing approximate solutions that are close to the optimal solution while significantly reducing computation time.

MILP focuses on finding optimal solutions for fixed parameters that most modern solvers efficiently handle. In contrast, mp-MILP extends this by exploring how varying sensitivity parameters influence solutions over a range, making it significantly more complex. mp-MILP requires mapping the relationships between changing parameters and their impact on solutions. It is a process beyond the capacity of tools like MPT3, which are limited to handling simpler scenarios with fewer variables. Unlike the previous parametric analysis methods, this research includes a large number of binary variables in the SCUCED problem, better reflecting the transmission line capacity upgrades and ISOs' goal of minimizing system costs. Therefore, we assess the economic value of transmission expansion under both normal and extreme conditions.

6. Conclusion and Future Work

This is the first study to use parametric analysis for multi-period MILP to address TEP challenges, specifically tailored to address ISO's multiple-period SCUCED problems. This study considers realistic modeling in transmission upgrade problems, which includes starting ramp rate restrictions, ramp-up rate limits, ramp-down limits, and shutdown constraints. This paper presents a novel approach for performing large-scale MILP parametric analysis using the B&B method to facilitate the solution process by investigating the upper and lower bounds to achieve the best approximate solution for multiple periods of SCUCED parametric analysis problems with a large number of binary variables.

Increasing the existing transmission line capacity is a desirable technique for responding to development by countering instability and ensuring transmission-line security. The optimum upgrade policy for a transmission line planning problem that includes increasing the capacity of existing lines corresponds to ISO's perspective on which line capacity should be increased to reduce system production cost. This study characterizes this as an RHS uncertainty parametric analysis for the MILP. A new matrix approach is provided that employs the classical Lagrangian function and the B&B algorithm. The classic B&B approach is extended to efficiently produce approximate analytical solutions for large-scale MILP parametric analysis problems. At each node, the lower and upper bounds are compared, and if the error is smaller than a predefined tolerance range, the branching process ends, and the current upper bound becomes the final approximate solution. The proposed method is especially useful for solving multi-period and mp-MILP problems with transmission capacity uncertainty, which is a significant challenge in TEP.

By analyzing the analytically optimal system cost function and the potentially improved transmission capacity and comparing the cost-cutting rate to the capacity increase, decision makers can adopt realistic line capacity changes and achieve minimum system cost. As a result, transmission planners or the ISO must carefully balance the marginal benefits of additional line capacity with the cost of improving line capacity. Building new lines or increasing the transmission capacity of existing lines can help to relieve network congestion and maintain system security and stability. These new findings considerably contribute to this field of study and increase our knowledge of how to manage the expansion of transmission capacity.

In this paper, only the upgrading capacity of the current transmission line is considered. Future studies should address establishing additional lines (TEP problem) by adding new branches and adjusting the generation shift factor (GSG) in the left-hand constraint matrix. It would also be worthwhile to identify suitable energy storage for upgrading or adding capacity, which will help relieve congestion and reduce total system costs. In addition, we are planning to develop sophisticated algorithmic packages for the parametric analysis of large-scale data systems. This initiative aims to advance the theoretical foundations and enhance the practical applications of mp-MILP, addressing the complexities of modern energy systems. The results of this study are based on the assumption that generators have linear generation costs. However, it is recognized that this linear modeling does not capture the more precise and realistic non-linear objective relationships in electricity generation costs, as demonstrated by Sioshansi [76] and Hua and Baldick [77]. Recognizing this limitation, we propose to explore advanced modeling techniques that incorporate piecewise linear and non-linear objective functions in future work. We are aware that integrating such functions into the mp-MILP framework introduces significant challenges, including increased model complexity, more intricate parameter space partitioning, and limitations of current solvers in handling the expanded problem size. Addressing these challenges requires developing new algorithms and solution methods. Such enhancements aim to improve the applicability and accuracy of our models across various real-world contexts. We need to consider how the transmission network expansion and cost allocation are set for the two scenarios to maximize decision-makers' profit. We also investigate the importance of extreme weather and tail events in assessing transmission expansion value.

Acknowledgments

This research is based upon work supported by the US Department of Energy's Office of Energy Efficiency and Renewable Energy (EERE) under the Water Power Technologies Office (Grant no. DE-EE0008781) and the National Science Foundation Award no. 2339956. The views expressed herein do not necessarily represent the views of the U.S. Department of Energy or the United States Government.

References

[1] IRENA. 2024. *Renewable energy highlights*. Available at: https://www.irena.org/-/media/Files/IRENA/Agency/Publication/2024/Jul/Renewable_energy_highlights_FINAL_July_2024.pdf

[2] Bird L., Milligan M., Lew D. (2013). Integrating Variable Renewable Energy: Challenges and Solutions. Technical Report. https://dx.doi.org/10.2172/1097911

[3] Mays J. (2023). Generator Interconnection, Network Expansion, and Energy Transition. *IEEE Transactions on Energy Markets, Policy and Regulation*, 1(4): 410-419.

[4] Brown H.E., Suryanarayanan S., Natarajan S.A., Rajopadhye S. (2012). Improving reliability of islanded distribution systems with distributed renewable energy resources. *IEEE Transactions on Smart Grid*, 3 (4), 2028-2038.

[5] Menghwar M., Yan J., Chi Y., Amin M. A., Liu Y. (2024). A market-based real-time algorithm for congestion alleviation incorporating EV demand response in active distribution networks. *Applied Energy*, 356, 122426.

[6] Uzum B., Yoldas Y., Bahceci S., Onen A. (2024). Comprehensive review of transmission system operators–Distribution system operators collaboration for flexible grid operations. *Electric Power Systems Research*, 227 (Part A), 109976.

[7] Alanazi M., Mahoor M., Khodaei A. (2020). Co-optimization generation and transmission planning for maximizing large-scale solar PV integration. *International Journal of Electrical Power & Energy Systems*, 118, 105723.

[8] Qiu T., Xu B., Wang Y., Dvorkin Y. and Kirschen D.S. (2017). Stochastic Multistage Co-planning of Transmission Expansion and Energy Storage. *IEEE Transactions on Power Systems*, 32(1), 643-651.

[9] Ugranli F., Karatepe E. (2016). Transmission Expansion Planning for Wind Turbine Integrated Power Systems Considering Contingency. *IEEE Transactions on Power Systems*, 31(2),1476-1485.

[10] Muñoz F., Torres F., Martínez S., Roa C., García L. (2019). Case study of the increase in capacity of transmission lines in the Chilean system through probabilistic calculation model based on dynamic thermal rating. *Electric Power Systems Research*, 170, 35-47.

[11] González F. F., Sauma E., Hendrik A. (2022). Community energy projects in the context of generation and transmission expansion planning. *Energy Economics*, 108, 105859.

[12] Baldick B, O'Neill R. P. (2009). Estimates of Comparative Costs for Uprating Transmission Capacity. *IEEE Transactions on Power Systems*, 24(2),961-969.

[13] Sebastian O. H., Muñoz J., Fredes F., Sauma E. (2022). Impact of increasing transmission capacity for a massive integration of renewable energy on the energy and environmental value of distributed generation. *Renewable Energy*,183, 524-534.

[14] Larruskain D. M., Zamora I., Abarrategui O., Iraolagoitia A. M., Gutiérrez M. D., Loroño E., Bodega F. D. (2006). Power transmission capacity upgrade for overhead lines. *Renewable Energy and Power Quality Journal*, 1, 221-227.

[15] Larruskain D. M., Zamora I., Abarrategui O., Aginako Z. (2011). Conversion of AC distribution lines into DC lines to upgrade transmission capacity. *Electric Power Systems Research*, 81(7),1341-1348.

[16] Manickam R., Palaniappan S. N. (2018). Upgrading transmission line capability by AC–DC conversion. *Computers & Electrical Engineering*, 68, 616-628.

[17] Morquecho E.G., Torres S.P., Matute N.E., Astudillo-Salinas F., Lopez J.C., Flores W.C. (2020). AC Dynamic Transmission Expansion Planning using a Hybrid Optimization Algorithm. *2020 IEEE PES Innovative Smart Grid Technologies Europe (ISGT-Europe)*, The Hague, Netherlands, 499-503.

[18] Sehloff D., Roald L.A. (2022). Low Frequency AC Transmission Upgrades with Optimal Frequency Selection. *IEEE Transactions on Power Systems*, 37(2), 1437-1448.

[19] Mbuli N., Xezile R., Motsoeneng L., Ntuli M., Pretorius J. (2019). A literature review on capacity uprate of transmission lines: 2008 to 2018. *Electric Power Systems Research*,170, 215-221.

[20] Mays J., Craig M. T., Kiesling L., Macey J. C., Shaffer B., Shu H.(2022). Private risk and social resilience in liberalized electricity markets. *Joule*, 6(2): 369-380.

[21] Millstein D., Wiser R., Gorman W., Jeong S., Kim J., Ancell A. (2022). Empirical Estimates of Transmission Value using Locational Marginal Prices. Lawrence Berkeley National Laboratory. August 2022. Available at: https://eta-publications.lbl.gov/sites/default/files/lbnl-empirical_transmission_value_study-august_2022.pdf

[22] Guo C., Bodur M., Papageorgiou D. J. (2022). Generation expansion planning with revenue adequacy constraints. *Computers & Operations Research*, 142,105736.

[23] Min D., Ryu J., Choi D. G. (2018). A long-term capacity expansion planning model for an electric power system integrating large-size renewable energy technologies. *Computers & Operations Research*, 96, 244-255.

[24] Chen, Y. H., J. Li. (2011). Comparison of security constrained economic dispatch formulations to incorporate reliability standards on demand response resources into Midwest ISO co-optimized energy and ancillary service market. *Electric Power Systems Research*, 819, 1786-1795.

[25] Soofi A. F., Manshadi S. D. 2022. Strategic bidding in electricity markets with convexified AC market-clearing process. *International Journal of Electrical Power and Energy Systems*, 141, 108096.

[26] Li F. (2007). Continuous Locational Marginal Pricing (CLMP). *IEEE Transactions on Power Systems*, 22(4),1638-1646.

[27] Li F., Bo R. (2009). Congestion and Price Prediction Under Load Variation. *IEEE Transactions on Power Systems*, 24(2), 911-922.

[28] Ponciroli R., Stauff N. E., Ramsey J., Ganda F., Vilim R. B. (2020). An Improved Genetic Algorithm Approach to the Unit Commitment/Economic Dispatch Problem. *IEEE Transactions on Power Systems*, 35(5), 4005-4013.

[29] Pluta M., Wyrwa A., Suwała W., Zyśk J., Raczyński M., Tokarski S. (2020). A Generalized Unit Commitment and Economic Dispatch Approach for Analysing the Polish Power System under High Renewable Penetration. *Energies*, 13, 1952.

[30] Fong S. L., Bucheli J., Sampath A., Bedewy A. M., Di Mare M., Shental O., Islam M. N. (2023). A Mixed-Integer Linear Programming Approach to Deploying Base Stations and Repeaters. *IEEE Communications Letters, 27*(12), 3414-3418.

[31] Hemmati R., Hooshmand R. A., Khodabakhshian A. (2014). Market based transmission expansion and reactive power planning with consideration of wind and load uncertainties. *Renewable and Sustainable Energy Reviews*, 29, 1-10.

[32] Russo L., Nair S. H., Glielmo L., Borrelli F. (2023). Learning for Online Mixed-Integer Model Predictive Control With Parametric Optimality Certificates. *IEEE Control Systems Letters*, 7, 2215-2220.

[33] Rivotti P., Pistikopoulos E. N. (2014). Constrained dynamic programming of mixed-integer linear problems by multi-parametric programming. *Computers & Chemical Engineering*, 70,172-179.

[34] Dua V., Bozinis N. A., Pistikopoulos E. N. (2001). A new multiparametric mixed-integer quadratic programming algorithm. *Computer Aided Chemical Engineering*, 9, 979-984.

[35] Oberdieck R., Wittmann-Hohlbein M., Pistikopoulos E. N. (2014). A branch and bound method for the solution of multiparametric mixed integer linear programming problems. *Journal of Global Optimization*, 59, 527-543.

[36] Liu Y., Jin S., Zhou J., Hu Q. (2023). A branch-and-bound algorithm for the unit-capacity resource constrained project scheduling problem with transfer times. *Computers & Operations Research*, 151, 106097.

[37] Charitopoulos V. M., Papageorgiou L. G., Dua V. (2018). Multi-parametric mixed integer linear programming under global uncertainty. *Computers & Chemical Engineering*, 116, 279-295.

[38] Feng Y. Q., Zhang F. Y., Xu J.W., He Z. X., Zhang Q., Xu K. J. (2023). Parametric analysis and multi-objective optimization of biomass-fired organic Rankine cycle system combined heat and power under three operation strategies. *Renewable Energy*, 208, 431-449.

[39] Dua V., Bozinis E. N., Pistikopoulos E. N. (2002). A multiparametric programming approach for mixed-integer quadratic engineering problems. *Computers & Chemical Engineering*, 26(4-5), 715-733.

[40] Gupta A., Bhartiya S., Nataraj P. S. V. (2011). A novel approach to multiparametric quadratic programming. *Automatica*,7(9), 2112-2117.

[41] Habibi J., Moshiri B., Sedigh A. K., Morari M. (2016). Low-complexity control of hybrid systems using approximate multi-parametric MILP. *Automatica*, 63, 292-301.

[42] Avraamidou S., Pistikopoulos E. N. (2017). A Multiparametric Mixed-integer Bi-level Optimization Strategy for Supply Chain Planning Under Demand Uncertainty. *IFAC-Papers Online*, 50(1), 10178-10183.

[43] Mate S., Bhartiya S., Nataraj P. S.V. (2020). Multiparametric Nonlinear MPC: A region free approach. *IFAC-Papers Online*, 53(2), 11374-11379.

[44] Shokry A., Medina-González S., Baraldi P., Zio E., Moulines E., Espuña A. (2021). A machine learning-based methodology for multi-parametric solution of chemical processes operation optimization under uncertainty. *Chemical Engineering Journal*, 425, 131632.

[45] Pappas I., Diangelakis N. A., Pistikopoulos E. N. (2021). Multiparametric/explicit nonlinear model predictive control for quadratically constrained problems. *Journal of Process Control*, 103, 55-66.

[46] Mahéo A., Belieres S., Adulyasak Y., Cordeau J. F. (2024). Unified Branch-and-Benders-Cut for two-stage stochastic mixed-integer programs. *Computers & Operations Research*, 164, 106526.

[47] Acevedo J., Pistikopoulos E. N. (1997). A multiparametric programming approach for linear process engineering problems under uncertainty. *Industrial & Engineering Chemistry Research*, 36(3), 717-728.

[48] Dua V., Pistikopoulos E. N. (2000). An Algorithm for the Solution of Multiparametric Mixed Integer Linear Programming Problems. *Annals of Operations Research*, 99, 123-139.

[49] Faísca N. P., Kouramas K. I., Pistikopoulos E. N. (2009). Global Optimization of mp-MILP Problems. *Computer Aided Chemical Engineering*, 26, 919-924.

[50] Gal T., Nedoma J. (1972). Multiparametric Linear Programming. *Management Science*, 18(7), 406-422.

[51] Mitsos A., Barton P.I. (2009). Parametric mixed-integer 0-1 linear programming: The general case for a single parameter. *European Journal of Operational Research*, 194(3), 663-686.

[52] Hladík M. (2010). Multiparametric linear programming: Support set and optimal partition invariancy. *European Journal of Operational Research*, 202(1), 25-31.

[53] Adelgren N., Wiecek M. M. (2016). A two-phase algorithm for the multiparametric linear complementarity problem. *European Journal of Operational Research*, 254(3), 715-738.

[54] Crema A. (1997). A contraction algorithm for the multiparametric integer linear programming problem. *European Journal of Operational Research*, 101(1), 130-139.

[55] Crema A. (2002). The multiparametric 0–1-integer linear programming problem: A unified approach. *European Journal of Operational Research*, 139(3), 511-520.

[56] Domínguez L. F., Pistikopoulos E. N. (2010). Multiparametric programming based algorithms for pure integer and mixed-integer bilevel programming problems. *Computers & Chemical Engineering*, 34(12), 2097-2106.

[57] ERCOT 2020. *ERCOT protocols section 4: Day-ahead operations*. Available at: http://www.ercot.com/mktrules/nprotocols/current

[58] PJM. 2019. *PJM Manual 11: Energy & Ancillary Services Market Operations Revision: 101*. Available at: https://www.pjm.com/-/media/training/nerc-certifications/gen-exam-materials-feb-18-2019/manuals/energy-and-ancillary-services-mkt-ops.ashx

[59] Carrion M., Arroyo J. M. (2006). A computationally efficient mixed-integer linear formulation for the thermal unit commitment problem. *IEEE Transactions on Power Systems*, 21(3),1371-1378.

[60] Lin C., Wu W., Chen X., Zheng W. (2018). Decentralized Dynamic Economic Dispatch for Integrated Transmission and Active Distribution Networks Using Multi-Parametric Programming. *IEEE Transactions on Smart Grid*, 9(5),4983-4993.

[61] Wang S., Zhao C., Fan L., Bo R. (2022). Distributionally Robust Unit Commitment with Flexible Generation Resources Considering Renewable Energy Uncertainty. *IEEE Transactions on Power Systems*, 37(6), 4179-4190.

[62] Zaman F., Elsayed S. M., Ray T., Sarker R. S. (2016). Evolutionary algorithms for power generation planning with uncertain renewable energy. *Energy*, 112, 408-419.

[63] Moarefdoost M. M., Lamadrid A. J., Zuluaga L. F. (2016). A robust model for the ramp-constrained economic dispatch problem with uncertain renewable energy. *Energy Economics*, 56, 310-325.

[64] Pravin P. S., Misra S., Bhartiya S., Gudi R. D. (2020). Advanced control of a reformer based fuel cell system coupled with multiple, uncertain renewable energy sources and an energy storage system. *IFAC-PapersOnLine*, 53(1), 374-379.

[65] Prajapati V. K., Mahajan V. (2021). Reliability assessment and congestion management of power system with energy storage system and uncertain renewable resources. *Energy*, 215, 119134.

[66] Vaskovskaya T., Thakurta P. G., Bialek J. (2018). Contribution of transmission and voltage constraints to the formation of locational marginal prices. *International Journal of Electrical Power & Energy Systems*, 101, 491-499.

[67] Kara G., Pisciella P., Tomasgard A., Farahmand H., del Granado P. C. (2022). Stochastic local flexibility market design, bidding, and dispatch for distribution grid operations. *Energy*, 253, 123989.

[68] Lara, C. L., Mallapragada, D. S., Papageorgiou, D. J., Venkatesh, A., & Grossmann, I. E. (2018). Deterministic electric power infrastructure planning: Mixed-integer programming model and nested decomposition algorithm. *European Journal of Operational Research*, 271(3), 1037-1054.

[69] Li, C., Conejo, A. J., Liu, P., Omell, B. P., Siirola, J. D., & Grossmann, I. E. (2022). Mixed-integer linear programming models and algorithms for generation and transmission expansion planning of power systems. *European Journal of Operational Research*, 297(3), 1071-1082.

[70] Gjorgiev, B., David, A. E., Sansavini, G. (2022). Cascade-risk-informed transmission expansion planning of AC electric power systems. *Electric Power Systems Research*, 204, 107685.

[71] Yin, X., Chen, H., Liang, Z., Zeng, X., Zhu, Y., Chen, J. (2023). Robust transmission network expansion planning based on a data-driven uncertainty set considering spatio-temporal correlation. *Sustainable Energy, Grids and Networks*, 33, 100965.

[72] Motta, V. N., Anjos, M. F., Gendreau, M. (2024). Survey of optimization models for power system operation and expansion planning with demand response. *European Journal of Operational Research*, 312(2), 401-412.

[73] El-Meligy, M. A., Sharaf, M. (2024). Robust transmission expansion planning under robust network constrained-unit commitment. *Electric Power Systems Research*, 229, 110164.

[74] Oberdieck, R., Diangelakis, N. A., Papathanasiou, M. M., Nascu, I., & Pistikopoulos, E. N. (2016). Pop–parametric optimization toolbox. *Industrial & Engineering Chemistry Research*, 55(33), 8979-8991.

[75] Herceg, M., Kvasnica, M., Jones, C. N., Morari, M. (2013). Multi-parametric toolbox 3.0. *In 2013 European control conference (ECC)* (pp. 502-510). IEEE.

[76] Sioshansi, R. (2014). When energy storage reduces social welfare. *Energy Economics*, 41, 106-116.

[77] Hua, B., Baldick, R., Wang, J. (2017). Representing operational flexibility in generation expansion planning through convex relaxation of unit commitment. *IEEE Transactions on Power Systems*, 33(2), 2272-2281.